DESIGN AND FABRICATION OF NEURAL CULTURE STRUCTURES FOR MONITORING OF NEURAL IMPLANT PERFORMANCE

by

Bengü Aktaş

B.S., in Biochemistry, Ege University, 2011

M.S., in Biomedical Engineering, Boğaziçi University, 2014

Submitted to the Institute of Biomedical Engineering

in partial fulfillment of the requirements

for the degree of

Doctor

of

Philosophy

Boğaziçi University

2023

ACKNOWLEDGMENTS

I would like to express my gratitude and special thanks to my advisor, Prof. Dr. Bora Garipcan, for the continuous support during my PhD research. I would also like to thank my committee members, Assoc. Prof. Dr. Duygu Ege and Assoc. Prof. Dr. Sedat Odabaş, for their encouragement and valuable insights, as well as Prof. Lorenzo Moroni and Assoc. Prof. Dr Paul Wieringa for their invaluable support during my time as a visiting scientist at the Institute for Technology-Inspired Regenerative Medicine (MERLN) at Maastricht University in the Netherlands. Additionally, I extend my thanks to Prof. Sebastien Foulquier for guiding and supporting the cell studies conducted at the Department of Pharmacology-Toxicology, Maastricht University. And I would like to thank Assist. Prof. Dr. Mustafa Kemal Ruhi for the valuable guidance and insights that he provided throughout this journey.

I am also grateful to Alp Özgün, Hayriye Öztatlı, Morteza Teymoori and Özgen Öztürk Öncel, who supported me at every stage of this thesis. I extend a sincere thank you to Sezin Eren Demirbüken and Agâh Karakuzu for injecting humor into this academic journey, making it all the more enjoyable. Finally, I would also like to thank my laboratory colleagues for sharing their knowledge and for the fun we had together.

I would like to express my sincere thanks to my dear friends Ayşegül Tümer and Öznur Demir for consistently being there for me, brightening my days with their presence, and providing their support.

Most importantly, I am deeply grateful to my family for the unwavering support they have provided me throughout my life and during this challenging journey. Words cannot adequately convey my gratitude to them for the sacrifices they have made on my behalf.

This Ph.D. study was partially supported from grants provided by the Boğaziçi

University Research Fund (BAP) by Grant Numbers 14642 and 6701.

ACADEMIC ETHICS AND INTEGRITY STATEMENT

I, Bengü Aktaş, hereby certify that I am aware of the Academic Ethics and Integrity Policy issued by the Council of Higher Education (YÖK) and I fully acknowledge all the consequences due to its violation by plagiarism or any other way.

Name :

Signature:

Date:

ABSTRACT

DESIGN AND FABRICATION OF NEURAL CULTURE STRUCTURES FOR MONITORING OF NEURAL IMPLANT PERFORMANCE

Enhancing neuroprosthetic biocompatibility requires refining approaches to reduce side effects from invasive devices. Physical, chemical, and bioactive design aspects of biomaterials are proven to be important for providing proper cell-to-cell, cell-to-material interactions. Modifying neural implant surfaces with bioactive cues, particularly employing cell adhesion molecules, shows promise in creating efficient interfaces. Within this concept, this study utilized N-Cadherin, NCAM and the mixture (1:1) of these molecules with the aim of modifying representative gold electrode surfaces to enhance neuron-electrode contact. The study assessed modifications on both undifferentiated and differentiated neuroblastoma SH-SY5Y cell lines. Successful modifications demonstrated biocompatibility with cell viability results, and notably, surfaces modified with NCAM and N-Cad/NCAM outperformed traditional poly-L-lysine (PLL) coatings in supporting neurite growth. The subsequent part of the study also included a comparison between NCAM-modified surfaces and Collagen type I coated surfaces which was used as the negative control, alongside conventional poly-D-lysine (PDL)/laminin coated surfaces. This investigation aimed to elucidate behavior in C8D1A astrocyte cells, provide insight into glial scar formation, and suggest potential strategies to attenuate cell responses. The results underscored the dual impact of NCAM molecules on astrocyte behavior and the intricate response induced by Collagen type I, contributing to an optimized approach for understanding cellular actions in the local environment and the development of alternative neural interfaces.

Keywords: Au Surface, N-Cad, NCAM, Cell Adhesion Molecules, SH-SY5Y Neuroblastoma Cells, C8D1A Astrocyte Type I Clone Cells, Collagen Type I.

ÖZET

NÖRAL İMPLANT PERFORMANSININ İZLENMESİ İÇİN NÖRAL KÜLTÜR YAPILARININ TASARIMI VE FABRİKASYONU

Nöroprostetiklerin biyouyumluluğunun artırılması, girişimsel cihazlardan kaynaklanan yan etkileri azaltacak yaklaşımların iyileştirilmesini gerektirir. Biyomalzemelerin fiziksel, kimyasal ve biyoaktif tasarım özelliklerinin, uygun hücre-hücre ve hücre-malzeme etkileşimlerinin sağlanmasında önemli olduğu kanıtlanmıştır. Nöral implant yüzeylerini biyoaktif ipuçlarıyla modifiye etmek, özellikle hücre adezyon moleküllerinden yararlanmak, verimli arayüzler oluşturma konusunda umut vaat etmektedir. Bu konsept dahilinde, bu çalışma, nöron-elektrot temasını geliştirmek için temsili altın elektrot yüzeylerini modifiye etmek amacıyla N-Cadherin, NCAM ve bu moleküllerin karışımını (1:1) kullanmıştır. Çalışma, hem farklılaşmış hem de farklılaşmamış nöroblastoma SH-SY5Y hücre hatları üzerinde modifikasyonları değerlendirmiştir. Başarılı modifikasyonlar, hücre canlılığı ile biyouyumluluğunu kanıtlamış ve özellikle NCAM ve N-Cad/NCAM ile modifiye edilmiş yüzeyler, nörit büyümesini destekleme konusunda geleneksel poli-L-lizin (PLL) kaplamalardan daha iyi performans göstermiştir. Çalışmanın bir sonraki kısmı, geleneksel poli-D-lizin (PDL)/Laminin kaplı yüzeylerin yanısıra, NCAM ile modifiye edilmiş yüzeyler ve negatif kontrol olarak kullanılan kolajen tip I kaplı yüzeyler arasında bir karşılaştırmayı da içermektedir. Bu araştırma, C8D1A astrosit hücrelerindeki davranışı aydınlatmayı, glial skar oluşumuna ilişkin bilgi sağlamayı ve hücre tepkilerini hafifletecek potansiyel stratejiler önermeyi amaçlamıştır. Sonuçlar, NCAM moleküllerinin astrosit davranışı üzerindeki ikili etkisinin ve kolajen tip I tarafından indüklenen karmaşık tepkinin altını çizerek, yerel ortamdaki hücresel eylemlerin anlaşılması ve alternatif sinir arayüzlerinin geliştirilmesi için optimize edilmiş bir yaklaşıma katkıda bulunmaktadır.

Anahtar Sözcükler: Au Yüzey, N-Cad, NCAM, Hücre Adezyon Molekülleri, SH-SY5Y Nöroblastoma Hücreleri, C8D1A tip I Klon Astrosit Hücreleri, Tip I Kolajen.

TABLE OF CONTENTS

LIST OF FIGURES

LIST OF TABLES

LIST OF SYMBOLS

Al-Kα	K-alpha X-rays of aluminum
eV	electrovolt
g force (RCF)	relative centrifugal force
mg	milligram
mL	milliliter
mM	millimolar
°C	degree Celcius
μg	microgram
μL	microliter
μm	micrometer

LIST OF ABBREVIATIONS

ANOVA	Analysis of Variance
ABIs	Acquired Brain Injuries
Au	Gold
BBB	Blood Brain Barrier
BCIs	Brain-Computer Interfaces
BMIs	Brain-Machine Interfaces
BSA	Bovine Serum Albumin
C8D1A	Astrocyte Type I Clone
$CaCl_2$	Calcium Chloride
Ca^{2+}	Calcium Ions
CAMs	Cell Adhesion Molecules
$CaSO_4$	Calcium Sulfate
Col I	Collagen Type I
CSPG	Chondroitin Sulphate Proteoglycan
CNS	Central Nervous System
DAPI	4,6-diamidino-2-phenylindole
DBS	Deep Brain Stimulation
DMEM	Dulbecco's Modified Eagle Medium
DMSO	Dimethyl Sulfoxide
ECM	Extracellular Matrix
FBR	Foreign Body Response
GFAP	Glial Fibrillary Acidic Protein
IL-1	Interleukin 1
IL-6	Interleukin 6
MCS	Motor Cortex Stimulation
N-Cad	Neural Cadherin (N-Cadherin)
NCAM	Neural Cell Adhesion Molecule
MEAs	Michigan Microelectrode Arrays

NI	Neural Interface
PBS	Phosphate Buffered Saline
PDL	Poly-D-lysine
PLL	Poly-L-lysine
PLL-P	Physically Modified Poly-L-Lysine
PLL-C	Chemically Modified Poly-L-Lysine
PNS	Peripheral Nervous System
sEEG	Stereo-electroencephalography
SH-SY5Y	Neuroblastoma Cells
SCS	Spinal Cord Stimulation
TNFα	Tumor Necrosis Factor Alpha
UEAs	Utah Microelectrode Arrays
WCA	Water Contact Angle
XPS	X-ray Photoelectron Spectroscopy

1. INTRODUCTION

1.1 Motivation

Invasive or penetrating neuroprosthetic and neuromodulatory devices are powerful tools towards the diagnosis or treatment of neurological conditions (e.g., epilepsy, Parkinson's disease, dementia), deficiencies (e.g., cognitive or hearing), and studying neurobiological processes [1–5]. Most of these devices, including micromachined microelectrodes, wire-based arrays, and polymer microelectrodes, work on the principle of delivering electrical signals to neurons or recording neuronal activity through local field potentials or action potentials [6–8].

The direct contact between the electrode and neurons allows for much more detailed and higher-resolution data acquisition in addition to stimulation of defined neuroanatomical regions compared to indirect methods such as electroencephalography and transcranial magnetic stimulation. Nevertheless, clinical and research applications of these devices still have substantial limitations due to biocompatibility issues, especially considering the long-term applications, in view of the complex interplay at electrode-tissue interfaces.

Various approaches applied to achieve successful brain-electrode interfaces by using techniques based on improving the biocompatibility of the material to achieve minimal neuronal loss and decreased gliosis as a result of the inflammatory reaction. Techniques to introduce biocompatible and long-term stable electrodes aimed to alter size, shape, roughness, and stiffness of the electrodes to alleviate adverse responses through closely mimicking the native tissue environment [7, 9, 10]. Alternatively, surface chemistry strategies such as incorporation of anti-inflammatory drugs and surface modification through the integration of bioactive molecules, including components from the extracellular matrix (ECM), neurotransmitters, neurotrophic factors, cell adhesion molecules (CAMs) have been observed to ameliorate destructive post-implantation re-

sponses, even the promotion of the growth and survival of neurons around the implant site [11–14].

Among these concepts, CAMs such as N-Cadherin, NCAM, L1 are attracting considerable interest as bioactive cues in the design of biomimetic neural coatings or as soluble factors for cell culture components due to their positive impact on axonal growth, guidance, neuronal regeneration, synapse formation, plasticity, and other developmental mechanisms [15–20].

Based on this concept, in this thesis the use of NCAM and N-Cadherin molecules and their synergistic effects as surface coatings to design optimized bio-interfaces are examined.

1.2 Objectives and Outline of the Thesis

The primary aim of this thesis is to enhance the biocompatibility of neuroprosthetics through surface modification with cell adhesion molecules. This effort is aimed at enhancing the interaction between cells and neural implants to mitigate neuronal loss and increase the likelihood of preventing long-term electrode failure. Furthermore, this research aims to assess the potential impact of these molecules on astrocytes with the goal of reducing gliosis.

To accomplish this goal, SH-SY5Y human neuroblastoma cells, both in their undifferentiated state and in the differentiated form exhibiting neuron-like behavior, were subjected to exposure to cell adhesion molecule modified surfaces. Specifically, N-Cadherin (N-Cad), neural cell adhesion molecule (NCAM), and a combination of these molecules in a 1:1 ratio was implemented as modifications on gold (Au) surfaces. The effects of these molecules were compared to a conventional modification method involving the use of poly-L-lysine molecules. The study encompassed the monitoring of surface characterization parameters in conjunction with the findings from cell culture experiments. Subsequently, a distinct section of the research was dedicated to a limited

investigation involving the C8D1A (astrocyte type I) cell line. In this phase, the goal was to observe the impact of NCAM-modified gold surfaces on this cell type and compare it to both conventional modification molecules and, specifically, collagen type I (Col I), which is known to increase in the presence of gliosis formation. The results were then compared to assess the effects of these substances in a 2D context. Specific objectives of this thesis include:

- Comprehensive literature review of neuroprosthetic and neuromodulatory devices, with a focus on invasive neural electrodes and their association with neuronal loss and glial scar formation.
- Discussion of device biocompatibility, strategies for enhancing it, and the significance of cell adhesion molecules within this context.
- Investigating the impact of specified cell adhesion molecules on representative neural electrode surfaces by observing their effect on SH-SY5Y cell behavior *in vitro* and presenting data to demonstrate the biocompatibility of the modified surfaces.
- Investigating the impact of NCAM molecules on representative neural electrode surfaces by observing their effects on C8D1A cell behavior *in vitro* and comparing these effects with conventional modification methods and the Col-I glial scar indicator.

2. BACKGROUND

2.1 Neuroprosthetic and Neuromodulatory Devices

Neuroprosthetics represents an interdisciplinary field that bridges neuroscience and engineering approaches, with a focus on utilizing technological interventions to replace or modulate the function of the compromised nervous system or sensory organs, addressing disruptions caused by neurological disorders or injuries [21, 22]. Neuromodulation is also another concept intertwined with neuroprosthetics, representing a dynamically evolving domain with the aim of altering the neural activity for therapeutic purposes, and it consistently broadens its scope with a growing array of treatments and applications [23, 24]. These technologies possess the capability to interface with different segments of both the central nervous system (CNS) and peripheral nervous system (PNS). This is typically achieved by strategically placing electrodes next to the intended target cells or tissues.

As an example of these devices, stereo-electroencephalography (sEEG) plays a crucial part in the treatment of drug-resistant epilepsy. It employs depth electrodes to aid in the detection and precise localization of seizure activity within the brain [25]. Deep brain stimulation (DBS), an intervention that entails the implantation of stimulating electrodes into the brain, is utilized for conditions such as dystonia, essential tremors, or Parkinson's disease. Additionally, DBS exhibits promise in its potential applications for various other conditions [26]. Motor cortex stimulation (MCS) and spinal cord stimulation (SCS) stand as another efficacious approaches for managing neuropathic pain [27, 28]. Another advancement in this field also encompasses the integration of brain-computer interfaces (BCIs) or brain-machine interfaces (BMIs). These interfaces acquire brain signals and then process them to generate commands that are transmitted to an output device, facilitating the execution of a desired action [29]. In summary, these neurotechnological devices hold the potential to offer valuable insights into a wide range of conditions, including acquired brain injuries (ABIs),

neurological disorders, and neurobiological processes.

The neurotechnological devices function based on the principle of transmitting electrical signals to neurons or recording neuronal activity through local field potentials or action potentials. This is achieved through the utilization of electrodes which usually consist of an array of small conductive materials. These electrodes encompass various types, including micromachined microelectrodes, wire-based arrays, and polymer microelectrodes, which are integrated into the main devices [1, 6–8]. Figure 2.1 provides examples of these electrodes.

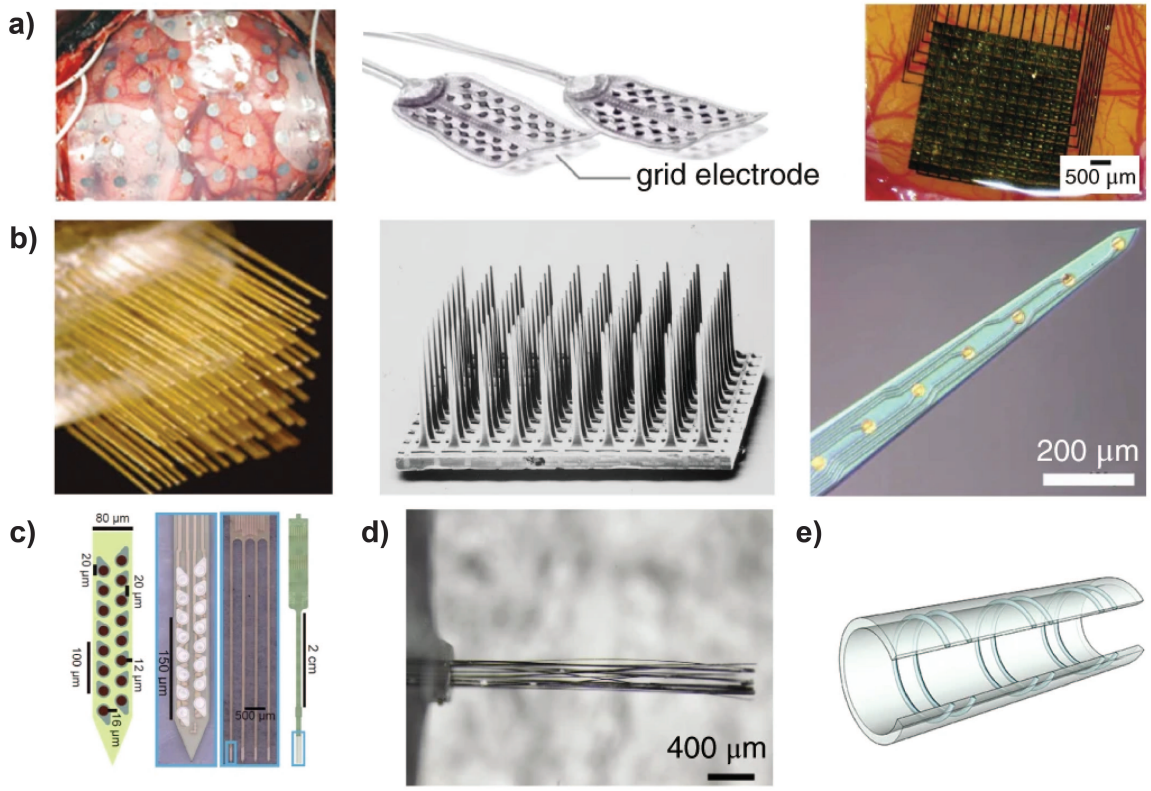

Figure 2.1 Neural electrode samples. a) commonly used non-penetrating invasive electrodes for ECoG recording, b) invasive microelectrodes, namely, Utah array and Michigan array, arranged from left to right, respectively., c) flexible penetrating polymer electrodes. d) carbon fiber electrode e) non-penetrating peripheral cuff electrodes. Reprinted from [30] with permission. Copyright 2020 by Springer Nature.

Direct contact between the electrode and neurons, facilitated by implantable or invasive electrodes, enables significantly more detailed and higher-resolution data

acquisition. This approach also allows for the precise stimulation of defined neuroanatomical regions, setting it apart from indirect methods. These systems demonstrate credible performance during acute recordings. However, they exhibit unreliable functionality in chronic settings. Hence, despite the advancement achieved in neuroelectronic devices, their widespread adoption frequently encounters challenges arising from electrode-related issues. These issues encompass the selection of materials, fabrication techniques, surface characteristics and shape, compatibility with tissue and the surgical procedures involved in the implantation process. The major failure generally stems from the foreign body reaction of tissue against electrode arrays, highlighting the paramount importance of biocompatibility in the design of implanted electrodes.

2.2 Neural Electrode-Induced Glial Response in Brain Tissue

The main problem of using invasive and penetrating electrodes is evoking a foreign body response (FBR) around the electrode interface (Figure 2.2), which is detrimental for the surrounding tissue and can further lead to impairment of signal quality and even mechanical failure of the electrodes as well [31, 32].

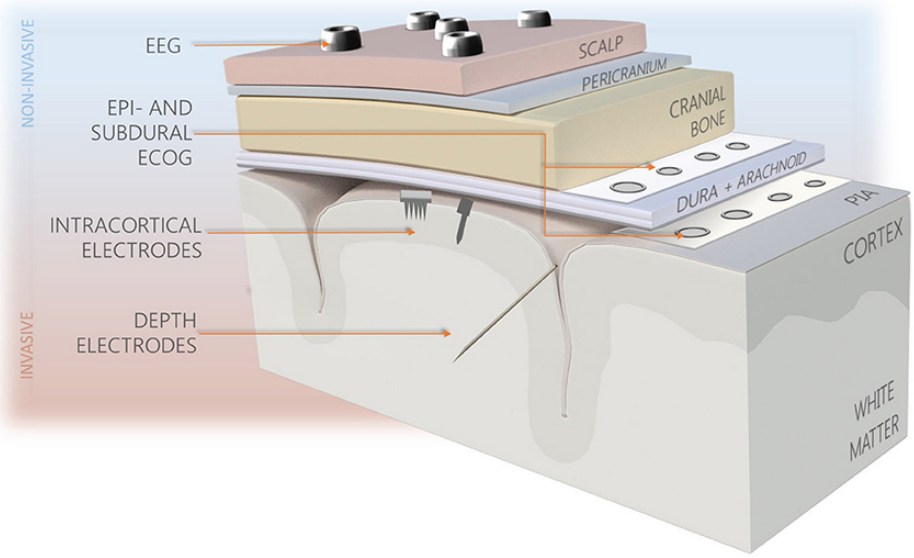

Figure 2.2 Classification of electrodes focusing on the central nervous system (CNS) and their respective positions [1].

Along with the placement of implantable electrodes, brain tissue attempts to isolate this exogenous material through a neuroinflammatory cascade mechanism. Following the impairment of the blood-brain barrier (BBB) through the insertion of electrode, blood serum proteins and complement factors absorb to the material surface, which in turn activates the inflammatory reaction of nearby glial cells [33, 34]. Among these glial cells, microglial cells start to encapsulate the electrode and release excitatory and proinflammatory factors (e.g., IL-1, IL-6, and TNFα) which cause to leave astrocytes their quiescent (resting) state and become activated, and recruit astrocyte over this thin encapsulation sheath [34–36].

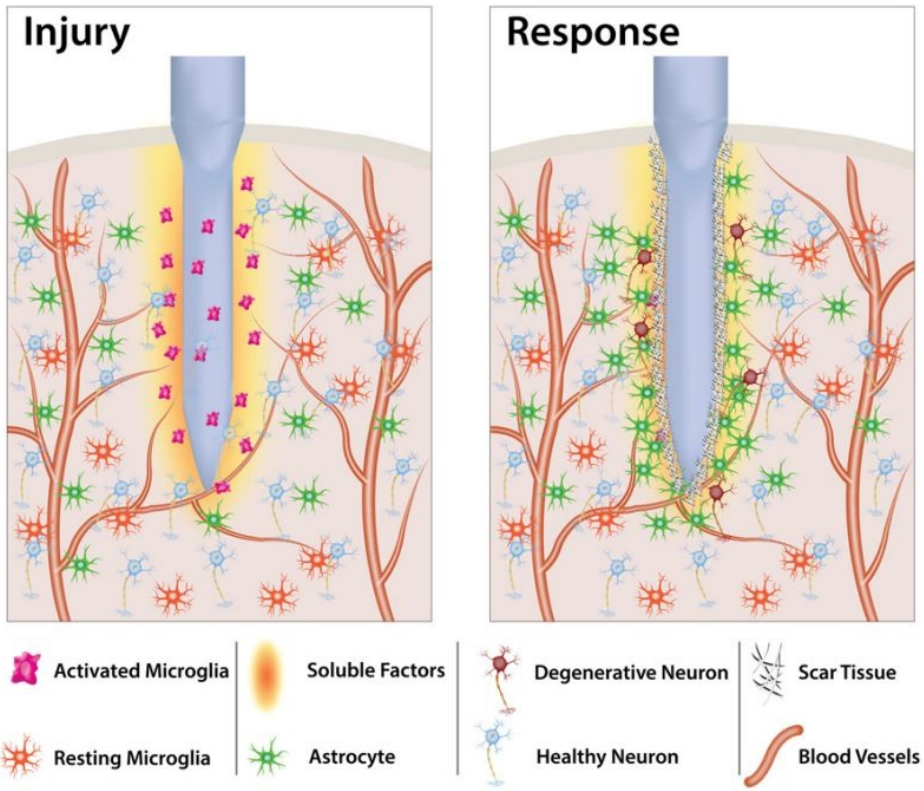

Figure 2.3 Formation of gliosis after neuroelectrode implantation. Readapted from [37] with permission. Copyright 2014 by Elsevier.

A compact layer of these reactive astrocytes reacts to injury by showing some characteristics such as hypertrophy, proliferation, increased production of glial fibrillary acidic protein (GFAP), vimentin, nestin and upregulation of extracellular substances especially chondroitin sulphate proteoglycans (CSPG) and tenascin which contribute to the formation of dense glial scar surrounding the implant [36, 38, 39]. This neuroprotective mechanism of astrocytes with aiming to minimize initial damage of CNS injury

is called 'reactive gliosis' or 'astrogliosis' [37, 40]. However, the intensified glial scar restrains the contact of neurons with the recording parts of electrodes and hampers ion exchange and neurotransmitter conduction, which in turn emerges as increased impedance, signal deterioration and electrode failure, especially in the final stage of the long term chronic inflammatory response. Likewise, neuronal cell degeneration and death occurs within 10 to 150 µm of the implant as this physical barrier is detrimental and toxic to local cells [7, 31, 41, 42].

The factors mentioned above continue to limit the widespread use of these devices in clinical and research settings, particularly for long-term applications. Consequently, there is a need for strategies to mitigate the adverse effects of invasive neuro-implants, thus enhancing their biocompatibility with the surrounding tissue.

2.3 Neural Interfaces and Strategies to Enhance Biocompatibility of Neuroelectronic Devices

Considering that the tissue reaction revolves around the neural interface (NI), serving as a platform for transmitting information amongst the nervous system and the electrode, a growing number of approaches have been developed to establish effective interfaces between electrodes and the brain [43]. These approaches aim to explore the biological aspects of gliosis mechanisms, for which the exact mechanisms are yet to be fully elucidated, with the objective of reducing the inflammatory reaction, ultimately preventing neuronal loss around the implant site.

Methods for developing chronically stable electrodes have focused on modifying electrode size, shape, roughness, and stiffness to mitigate adverse responses by closely mimicking the tissue environment [9, 10, 44]. Concurrently, research in the field of electrode design and construction has been making significant progress [45].

The materials used in the manufacture of electrodes are typically classified into

two primary categories: electrode and substrate materials. The construction of electrodes frequently utilizes noble metallic materials as recording sites and interconnections, including gold, platinum, stainless steel, tungsten, iridium, or platinum-iridium alloys which have been also employed as wire-based arrays since the early stages of electrode development owing to their outstanding electrical conductivity, chemical stability, and interfacing deeper brain areas [46, 47]. Nonetheless, these electrodes face limitations related to bending during insertion, a limited recording site confined to the tip of the electrode, an inability to precisely determine location, and the disparity between rigid structure and the soft nature of neural tissue. However, they are more likely to offer extended functionality compared to other electrodes while causing less damage to the nearby cellular environment. Later, silicon-based micromachined electrode arrays, represented by Michigan (MEAs) and Utah microelectrode arrays (UEAs), emerged as the next generation of electrode technology, thanks to the development of photolithography methods. These arrays provide advantages including high precision in achieving minimal sizes, high-density recording sites, the ability to spatially design neural activity, and large-scale manufacturing. Yet, the electrodes can only be utilized for short implantation periods due to concerns related to recording loss, and they still share the same primary drawback with wire-arrays, namely, the occurrence of foreign body response (FBR) [48, 49]. The 2D geometry of Michigan planar electrode arrays were believed to contribute to issues due to increased susceptibility to biotic fluids and glial encapsulation. To address this challenge, insulation is provided through the use of multiple layers of substrate materials, such as oxides, nitrides, and supplemented by an additional polymer layer.

Around the 1990s, Utah electrode arrays (UEA) emerged as a dependable choice for electrodes employed in chronic applications. These electrodes feature a bulk micromachined design, comprising 3D arrays equipped with recording sites at their tips. It is ideal for monitoring extensive neuronal activity; nonetheless, the examination frequently discloses the existence of microhemorrhages and the emergence of glial tissue encapsulation near the electrode tips post-implantation. In the long term, the quality of recorded signals ultimately deteriorates, with a significant reduction by half over time.

The material choices in the manufacture of both MEAs and UEAs, includes solid substrate materials like alumina, ceramic, diamond, glass, metal, silicon oxide, silicon nitride and silicon carbide (SiC), in addition to soft materials or polymer coatings such as SU-8, liquid crystal polymers (LCP), polyimide, parylene, and polydimethylsiloxane (PDMS) [45, 50–58]. Precisely transferring geometric shapes onto substrates to ensure compatibility with neural tissue is essential for the creation of the electrodes. Photolithography and its variations are key players in the fabrication process. However, they pose challenges when applied to intricate three-dimensional and high aspect ratio Utah electrode arrays (UEAs).

The polymers are also designed to address the mechanical mismatch issues often observed in silicon-based and microwire electrode arrays. These coatings can be mechanically customized to closely align with the properties of neural tissue. This flexibility mitigates the likelihood of significant strain, thereby reducing the potential for secondary inflammation. However, these materials come with challenges, including difficulties with *in vivo* adhesion, and a tendency to absorb water, leading to issues like delamination [45, 53]. These problems can also alter the electrical performance of the probes over time, constraining the use of these flexible electrode arrays to short-term or acute neural recordings [1].

Furthermore, the flexible and soft nature of these materials presents difficulties during the implantation process, particularly when applied in deeper regions of the brain. Many polymeric neural implants share similarities with silicon-based counterparts in that they feature multiple recording sites comprised of thin metal films like gold or platinum along the length of the shank. These implants can be further enhanced through the incorporation of conductive polymers (CP). Thanks to the material's structure and fabrication capabilities, they can accommodate a broader range of 2D or 3D geometric shapes, such as fishbone, mesh, or sinusoidal configurations. Additionally, they can also be combined with other materials, such as carbon nanotubes and nanoparticles, and can be functionalized with anti-inflammatory drugs and bioactive molecules [55, 56, 59–61].

The polymers can serve dual roles, functioning both as substrates and encapsulation materials. Some of the frequently employed polymers in this context include polyimide, parylene-C, benzocyclobutene (BCB), LCP, and SU-8. They are preferred for their inert characteristics and minimal dielectric constants, and their ability to resist moisture permeation making them suitable for neural implant applications. Additionally, these polymers offer the advantage of being easily functionalized with various organic agents to meet specific implant requirements.

Cutting-edge developments in neural electrode technology involve the fabrication of multimodal probes using polymers and polymer-metal compounds, facilitating both electrical recording and optical stimulation. These probes are especially advantageous in applications like optogenetics [62].

Hydrogel coatings, such as alginate, fibrin, hyaluronic acid, and polyethylene glycol, have also gained attention as promising candidates for neural interfacing. These coatings possess mechanical properties similar to biological tissue, good biocompatibility, body-absorbable characteristics, and high-water content. They offer the potential to mitigate mechanical mismatches after implantation and they can be customized with drugs and bioactive substances or living cells to create a protective layer between the implant and brain tissue. Yet, a notable downside is the difficulty in precisely regulating their thickness over the course of time due to swelling properties, which can potentially exert pressure on nearby tissue and lead to an increased separation between the electrode recording sites. Moreover, hydrogel-coated probes that are excessively smooth run the risk of the layer being removed upon insertion [54].

The mechanical properties, encompassing the shape and dimensions of the implants, play an essential role in influencing their overall performance and longevity within the neural environment, prompting significant research efforts to explore their influence on functionality and operational efficiency. Therefore, interfacial modification materials such as metals, metal oxides, carbon-based materials, and conductive polymers have also garnered significant attention in recent years owing to their advantageous properties and manufacturing feasibility [45]. It's crucial to emphasize that a

reciprocal correlation exists between the dimensions of recording sites and impedance. Smaller electrodes tend to generate more noise, exhibit lower recording quality which stems from a decrease in the maximum attainable stimulating current. One approach involves enhancing the geometric effective surface area of these implants through methods such as surface roughening and the application of materials like gold particles, carbon nanotubes, platinum black, and platinum grass. This not only amplifies the available surface area but also ensures the compactness of the recording site [63, 64]. In the study conducted by Chung and colleagues, they investigated the impact of CF_4 plasma treatment on gold electrodes incorporated into polyimide-based neural probes. Their findings revealed a significant outcome, with the roughening process resulting in an impressive 98% reduction in impedance [63, 65, 66]. Carbon nanotubes (CNTs), which consist of graphene sheets formed into cylinder structures, have also attracted considerable attention, especially owing to their high surface area, impressive mechanical and electrical properties, and their capacity for surface functionalization [53, 55, 67]. In the research of Sim *et al.*, it was demonstrated that vertically aligned carbon nanotubes (VACNTs) had a substantial positive effect on the recording capabilities of the neural probe. These VACNTs exhibited the lowest area-specific impedance when compared to black platinum electrodes [68]. Similar to CNTs, the outstanding high conductivity, transparency and flexibility properties of graphene also make it suitable for use with flexible substrates, thereby promoting conformal contact [69]. These materials can also exhibit functionalization properties, thereby potentially increasing their compatibility with tissue. Nevertheless, concerns regarding the toxicity of these materials remain. Researchers have also pursued the enhancement of electrode performance in micromachined electrode and microwire arrays through the development of metallic electrode derivatives, such as iridium oxide [1]. For instance, thin microwire arrays, which inherently possess higher impedance, can be fine-tuned using these derivatives to reduce their impedance in recording sites [70–73]. Conductive polymers (CPs), when combined with suitable dopants, also demonstrate remarkable electrical conductivity. In this context, the prevailing conductive polymers of choice are poly (3,4-ethylenedioxy thiophene) (PEDOT) and polypyrrole (PPy), alongside additional options like polyaniline (PANI) and poly(thiophene) (PT). These CPs can be further customized by inclusion of large dopants involving paratoluene sulfonate (pTS) or poly (styrene sulfonate) (PSS) to

finely tune their characteristics [54, 74, 75]. CPs are often combined with nanomaterials, hydrogels, or elastomers to tackle issues linked to their high elastic moduli, which can lead to detachment over extended periods of electrical stimulation [56, 76–78]. Additionally, they are combined with bioactive molecules to stimulate cellular responses [79, 80].

Lastly, regarding probe insertion, it's important to emphasize that the technique used for securing the probe plays a pivotal role in aggravating irritation. Tethered probes cause more significant glial scar and local neurodegeneration compared to free-floating electrodes due to their reduced mechanical flexibility. Furthermore, tethering has been observed to modify the shape and dimensions of the implantation site, compress neurons at the probe interface, and can serve as potential entry points for infections through the establishment of transcranial and percutaneous connections [81].

Following the manufacturing process, all implantable devices may undergo further refinement with the aim of regulating inflammatory responses, promoting neuronal growth in the vicinity of the implant site, and introducing new functionalities. This has been achieved through the attachment of various compounds to the devices, including anti-inflammatory drugs, or by utilizing surface chemistry techniques, particularly those involving bioactive molecules such as ECM components, neurotransmitters, neurotrophic factors, and cell adhesion molecules (CAMs) [11–14, 82, 83].

The effective administration of anti-inflammatory and neuroprotective agents has been demonstrated to reduce inflammation and oxidative stress. This promotes the integration of neural tissue with the implant by preventing neuronal damage near the electrodes, ultimately resulting in enhanced long-term recording quality [83, 84]. Controlled drug delivery can be applied concurrently with recording or stimulation in the target area, allowing for the precise exploration of metabolic mechanisms. Furthermore, drug delivery offers the advantage of reducing the long-term risk of infection. As an example, sulfonated silica nanoparticles (SNPs), employed as a conductive polymer dopant, were utilized in the electropolymerization of PEDOT films

and compared to PEDOT doped with polystyrenesulfonate (PSS). Nonporous SNPs-doped PEDOT films exhibited advantages such as reduced interfacial impedance, enhanced charge injection capabilities, and improved stability when contrasted with PEDOT/PSS. The use of porous SNP dopants introduced the capability to act as drug reservoirs, significantly enhancing the potential of electrically controlled drug release technology based on conducting polymers. Through the incorporation of SNP dopants, both drug loading and release capabilities were augmented, enabling the inclusion of cationic and electroactive compounds as potential drug candidates. Ultimately, the PEDOT/SNP composite demonstrated the ability to finely modulate *in vivo* neural activity through releasing a glutamate receptor antagonist in a controlled manner from microelectrode sites coated with the composite [85]. In another study, conductive polymer (CP) microcups (MCs) were fabricated to control the drug-loading/release characteristics and electrical properties of neural devices. For this purpose, monodisperse poly(lactide-co-glycolide) (PLGA) microspheres were electrosprayed on Au substrates and poly(pyrrole) (PPy) polymerization around PLGA microspheres was carried out with electrospraying method. Then, PLGA microsphere was dissolved and PPy MCs were obtained. They demonstrated the loading of an anti-inflammatory drug within PPy microstructures and its gradual release [86].

Biomimetic or nature-derived approaches can also play crucial role in resolving these challenges. For instance, materials such as ECM matrix proteins, peptides, polysaccharides, lipids, and nucleic acids have been utilized in biomedical research for many years. Collectively, their remarkable qualities, including biocompatibility, biodegradability without releasing toxic substances, physiochemical resemblance to biological tissue, reduced potential to provoke an immune response, position them as excellent candidates compared to synthetic materials for enhancing the biocompatibility and long-term safety of neural interfaces [82, 83]. These materials can be employed either as biocompatible coatings or as fundamental building blocks for neural interfaces. Within biocompatible coatings, the surface modified with these molecules functions as an interface buffer layer, effectively inhibiting the attachment of glia cells and immune system-triggering elements. These coatings should also create a supportive environment for the survival and growth of neuronal cells.

Within these concepts, polysaccharides such as agarose, chitosan, alginate, and dextran are intriguing examples of such materials due to their rheological properties, which closely resemble those of ECM glycosaminoglycans, and their low immunogenicity. In the study of Moon *et al.*, the researchers engineered nanofilms mimicking the ECM by employing a layer-by-layer (LbL) approach, wherein they combined ulvan (ULV) with chitosan polysaccharides. These nanofilms exhibited a remarkable ability to attach primary hippocampal neurons with significantly higher viability when compared to surfaces coated with poly-D-lysine. Furthermore, these nanofilms facilitated the growth of neuronal projections while concurrently inhibiting the attachment of astrocytes [87]. In a separate investigation, the researchers combined hyaluronic acid (HA), a common polysaccharide found in brain tissue with well-known anti-inflammatory properties, and polypyrrole (PPy) to produce electrode coatings. The PPy/HA coating successfully mitigated the inflammatory response and maintained consistent electrical performance over a span of three weeks [88]. Polysaccharides, known for their anticoagulant and anti-inflammatory properties, are continually under investigation as potential biointegrative coatings.

There are also studies using lipids aimed at engineering cell membranes to minimize cellular responses to implants, as well as research within the optogenetic field that employs nucleic acid components to facilitate gene transfer applications for cell modulation. Researchers synthesized supported lipid bilayers (SLBs) with varying lipid compositions and interacted them with primary neurons. A lipid called succinyl-PE was introduced to neuron-inspired biomembrane to expose phosphate (PO_4^-) groups. The succinyl carboxylate group made it possible to subsequently introduce negatively charged sulfonate groups. The research indicates that negatively charged SLBs could influence the elongation and branching of neurites, underscoring the potential of altering surface charge to affect neuronal processes [89]. In the study carried out by Huang *et al.*, a novel gene-embedded optoelectrode array was designed for neural implantation. This array enabled spatiotemporal electroporation (EP) for gene delivery and transfection, photomodulation, as well as simultaneous electrical monitoring of neural signals within the brain through a single implantation event. This was achieved by synthesizing a combined conductive hydrogel known as rGO/Amphiphilic Polysaccharide-Modified

PEDOT (PG) with organized nanodomains to encapsulate nonviral gene vectors referred to as PEI-NT-pDNA. Both *in vitro* and *in vivo* studies demonstrated that the PG-PEI-NT-pDNA combination effectively facilitated gene transfection into neurons. Moreover, when tested with the actual optogenetic opsin channel rhodopsin-2, the flexible neural probe incorporating an optical waveguide fiber exhibited photo-evoked spikes in the targeted brain regions [90].

Nature-derived proteins or ECM proteins, such as fibronectin, laminin, and various peptide fragments, are also extensively employed for similar purposes in neuroengineering research. In the quest to address material-induced neuroinflammatory limitations associated with intracortical microelectrodes, one of the initial strategies was to attach ECM proteins and peptides onto the implant surface. As an example of nature-derived materials, Kim *et al.* developed electrodes using a silk-covered bioresorbable film sourced from Bombyx mori cocoons onto an array of ultrathin polyimide (PI) electrodes and implanted three types of (PI array electrodes with a thickness of; 75 μm and 2.5 μm, reinforced by a silk layer, along with 2.5 μm silk mesh electrodes) in cats to record neural activity from the visual cortex. Among these, the 2.5 μm silk mesh electrode exhibited the best performance, with excellent channel contact and a higher signal-to-noise ratio (SNR). This approach, where the silk dissolves and resorbs after implantation, led to a conformal wrapping process without any observed immune response after a 4-week implantation period [91]. In the research conducted by Patil and colleagues, a pioneering method was employed, where silk was employed as an insulating layer resistant to water. The utilization of water annealing techniques achieved water-stable and nontransient silk neural interfaces, and the subsequent application of a conductive layer facilitated the development of flexible silk electrodes. The findings demonstrated that this electrode holds exceptional promise as a sensing interface for recording neural signals in both the cortex and peripheral nervous system [92]. In a separate study, CAS-IKVAV-S (IKV), a peptide derived from laminin, was covalently attached to polyimide sheets that had been functionalized with amino and vinyl groups. Two distinct coatings, namely PI_v+IKV and PI_a+IKV, were developed, and they were observed to enhance neuronal cell adhesion and neurite sprouting. Additionally, these coatings were found to support the viability of peripheral glial cells while mini-

mizing the presence of fibroblast contamination on the substrate [93]. Shen *et al.* also developed microelectrodes constructed from ECM proteins including collagen I (Col-I), Col-I/Col-IV, Col-I/laminin, and Col-I/fibronectin. They employed a combined system involving excimer laser micromachining and microtransfer-molding to create these microelectrodes. The final dimensions of these electrodes closely resembled those of silicon-based microelectrodes. *In vitro* recordings displayed that these ECM microelectrodes could capture neurologically relevant frequencies without causing significant alterations in their impedance characteristics. Furthermore, these microelectrodes exhibited high neuronal viability, providing support for neuronal cell bodies and neurites while also reducing neuroinflammation [94]. Additionally, studies began incorporating cell surface receptor proteins or cell adhesion molecules to facilitate more targeted cellular interactions.

As demonstrated by the examples, there is a range of design variations that encompass optimizing implant size, shape, and surface characteristics, along with the integration of bioactive molecules to modulate tissue responses. These designs can incorporate a combination of these elements or can be used alone. Despite multiple studies demonstrating the effectiveness of their approaches in reducing glial scar formation, the long-term stability of the coating remains a subject of debate due to certain reasons encompassing poor mechanical properties, continuous swelling upon water uptake of certain molecules, and instability of the molecules over time. These issues have the potential to lead to increased impedance over extended periods. Therefore, by employing a combinatory approach, the absent components can collaborate synergistically, gradually giving rise to the creation of an optimal probe capable of functioning across various aspects, including the suppression of immune responses and the accurate recording or transmitting of signals.

2.4 Cell Adhesion Molecules (CAMs) and Their Roles in Biocompatibility Strategies for Implantable Electrode Applications

CAMs are proteins situated on the cell surface that facilitate interactions, either between neighboring cells or between cells and the ECM. Trans interactions involving identical molecules are termed homophilic interactions, while those involving different molecules are referred to as heterophilic interactions. Functional investigations indicate that adhesion molecules play pivotal roles in various facets of neural network formation, encompassing axon guidance, synapse formation, synaptic structure regulation, and interactions between astrocytes and synapses. Once axonal growth cones have reached their intended target regions, they must still accurately identify the appropriate target cells to establish synapses. Subsequently, initial contacts are established between axons and dendrites, and the activation of both homophilic and heterophilic receptors initiates the development of synaptic specializations [95, 96].

Cell adhesion signifies a dynamic cellular process in which interactions lead to alterations in intracellular signaling, cytoskeletal arrangement, and/or gene expression. A multitude of adhesion molecules are actively engaged on the cell surface, while concomitantly, internal signaling systems within the cells persist in their operation. Additionally, interactions on the cell surface can be either adhesive or repulsive as a result of ongoing cellular processes. Consequently, the outcome largely relies on the spatially and temporally regulated net result of all CAM interactions taking place at the cell surface [95–97].

Cell adhesion molecules are typically grouped into five categories: cadherins, integrins, selectins, immunoglobulin superfamily (IgSF) including NCAM, nectins and other molecules such as mucins [98]. Among these groups, CAMs such as N-Cadherin, NCAM, and L1 have become the focus of research interest due to their influential role as bioactive cues in the design of biomimetic neural coatings. Moreover, these molecules are considered valuable soluble factors within cell culture components. They

exert a positive influence on various critical aspects of neural function, such as promoting axonal growth, providing guidance, facilitating neuronal regeneration, supporting synapse formation, enhancing plasticity, and contributing to other essential developmental mechanisms [15–20].

The molecules selected for this study, namely N-Cadherin and N-CAM, represent two of the major cell adhesion components distributed in the central nervous system [99]. N-Cadherin is a Ca^{2+} dependent and homophilic binding type glycoprotein that holds a pivotal position in neuronal cell adhesion, migration, and synaptic plasticity, and especially participates in the neurite formation and polarization mechanisms of cells by concentrating in synaptic junctions [100, 101]. NCAM is a Ca^{2+} independent cell-surface glycoprotein that belongs to Ig superfamily CAMs [102]. Like N-Cadherin, NCAM is also involved in regulating activities such as synapse formation and function, neurite extension, migration, etc. by forming homophilic or heterophilic interactions [103]. While both molecules play an important role in neuron survival, NCAM specifically inhibits astrocyte attachment or proliferation [104–106]. Haque *et al.* demonstrated that N-Cadherin coated polystyrene culture dishes promote the differentiation of embryonic stem cell and induced pluripotent stem cell (iPSC) derived neural progenitor cells (NPCs) in the absence of exogenous signals and stimulate neurite outgrowth further compared to poly-L-lysine (PLL) and gelatin coated surfaces [107]. Cherry *et al.* examined the impacts of N-Cadherin alone and L1-Fc combination-functionalized 2D films and 3D microfibrous scaffolds on H9 neural stem cells (H9-NSCs) and observed that low concentration of N-Cadherin in conjunction with higher L1 concentration enhanced neurite outgrowth and neuron related markers such as MAP2+ and NF [18]. NCAM has mostly been used as a soluble factor in different studies rather than as a coating component. Lagenaur and Lemmon used nitrocellulose coated petri dishes for non-covalent attachment of NCAM among several other protein samples for observing the neuron activity from chicken tecta and mouse cerebellum. However, they concluded that either nitrocellulose was unable to bind NCAM to petri dishes or NCAM did not play a major role in axon outgrowth of cells [108]. Later, Walsh *et al.* suggested that soluble NCAM chimeric molecules can stimulate neurite outgrowth from both rat and mouse cerebellar granule cells by activating the FGF receptor signaling

cascade [109]. Further studies have also demonstrated that soluble form or peptides constituting a part of NCAM induces the differentiation of cells to neuronal phenotype [110–113]. Besides these advances, Wiertz *et al.* observed that NCAM protein and antibody immobilization on polyethylene-imine (PEI) surfaces showed good neuronal adhesion on cerebral cortical neurons at high concentration (100 $\mu g/mL$), and neurons were also capable of attaching lower concentrations (3.0 $\mu g/mL$) of NCAM antibody, even though spreading was poor [114]. Considering the influences of these molecules on neuronal functions, more work related to their individual or synergistic effects could produce interesting findings for the optimization of neuroprosthetics.

3. CELL ADHESION MOLECULE IMMOBILIZED GOLD SURFACES FOR ENHANCED NEURON-ELECTRODE INTERFACES

In this part of thesis, the use of NCAM and N-Cadherin molecules and their synergistic effects as surface coatings to design optimized bio-interfaces were investigated. NCAM and N-Cadherin were covalently attached to gold (Au) surface, through crosslinker dithiobis (succinimidyl) propionate (DSP) [115]. Following characterization and confirmation of the covalent immobilization of the proteins, surfaces were assessed for biocompatibility by using SH-SY5Y neuroblastoma cell line. Furthermore, growth and differentiation of retinoic acid treated SH-SY5Y cells were investigated on surfaces modified with neural cell adhesion molecules. The findings show that the cell adhesion molecules, N-Cadherin, NCAM or the mixture of these molecules provided suitable environments regarding cell viability which demonstrated their biocompatible properties as coating materials. Furthermore, NCAM and N-Cad/NCAM crosslinked surfaces revealed promising improvements in neurite extension against standard PLL coatings that are conventionally used in neural studies. Overall, the results represent a step toward improving the fabrication of state-of-the-art neural-electronic platforms, especially for long-term applications.

3.1 Surface preparation and modification

Au-coated (50 nm) 15 mm borosilicate float glass coverslips (Hilgenberg-GmbH) were used for representing the recording site of the neural electrodes. The samples were sequentially cleaned with acetone (Merck, $\geq$ 99.0 %), ethanol (Isolab, $\geq$ 99.9 %), and deionized water (DI) in an ultrasonic bath and dried under a stream of nitrogen. Afterwards, they were transferred to a sterile biosafety cabinet and UV-sterilized for 15 min. For introducing N-hydroxysuccinimide (NHS) ester groups, gold surfaces were incubated in 4 mg/mL dithiobis(succinimidyl propionate) (DSP) (ThermoFisher Scientific, 22585) dissolved in dimethylsulfoxide (DMSO) (Genaxxon Bioscience GmbH)

for 30 min at RT. Following modification, unbound DSP was removed by rinsing with DMSO and then with water. Immediately after, surfaces were covalently functionalized for 2h at RT with N-Cadherin (Cloud-Clone Corp., RPB481Ra01), NCAM (LSBio, LS-G56413), or a 1:1 mixture of N-Cadherin/NCAM proteins at 5 μg/mL total protein concentration for all groups in phosphate buffered saline (PBS) (1X, pH 7.4). The functionalized surfaces were rinsed with PBS and prepared for characterization and cell culture experiments. Control surfaces were coated with 5 μg/mL Poly-L-lysine (PLL) (Sigma-Aldrich, P8920) in DI water either covalently (PLL-C) following DSP modification under the same conditions or physically (PLL-P) on cleaned surfaces in 37°C incubator for 2h. PLL adsorbed (PLL-P) surfaces were allowed to air dry. The schematic representation of surface modifications is shown in Figure 3.1.

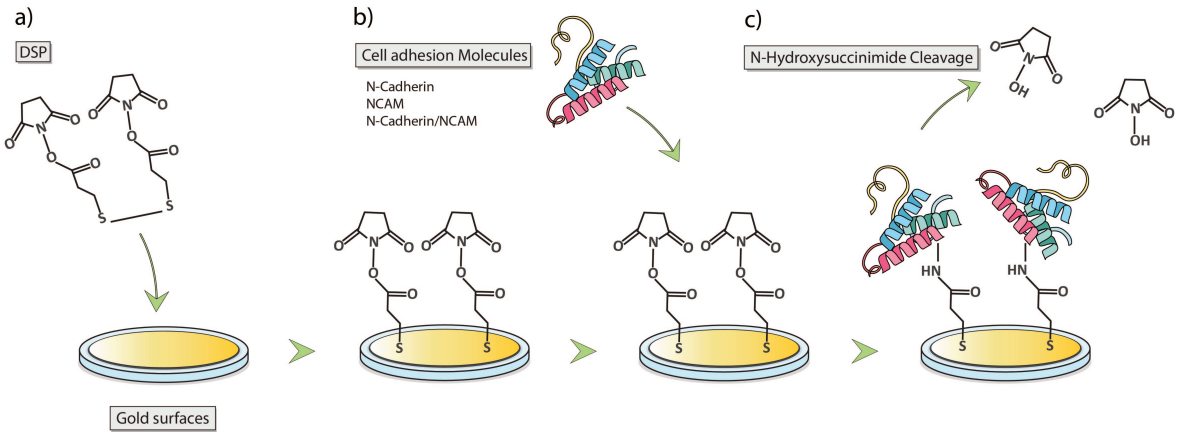

Figure 3.1 Covalent modification steps of gold surfaces with the specified cell adhesion molecules. a) Functionalization of gold surfaces with DSP (dissolved in DMSO) crosslinker after cleaning step, b) Covalent modification with N-Cadherin, NCAM, or N-Cad/NCAM (1:1) mixture in PBS immediately after DSP modification, c) Cleavage of N-hydroxysuccinimide (NHS) groups after reaction of DSP with the specified cell adhesion molecules.

3.2 Surface Characterization

3.2.1 Water Contact Angle Measurement

A sessile drop method was used to measure the wettability of the surfaces (CAM-100, KSV Instruments). Each 2 μL of DI water was carefully applied on three random regions of each modified and non-modified gold surface at RT. Following deposition, the droplets were recorded for 10s and the water contact angle (WCA) values were automatically calculated by fitting the captured drop images.

3.2.2 X-ray photoelectron spectroscopy (XPS)

Surface modifications were confirmed by characterizing samples with X-ray photoelectron spectrometer (XPS) (K-Alpha™+ XPS, Thermo Scientific) equipped with a monochromatic Al-KαX-Ray source, and 128-channel detector with 400 μm spot size. High-resolution spectra were obtained with a pass energy of 30 eV. The corresponding binding energies of specific chemical bonds were obtained according to the C1s peaks and N1s peaks. Peak fitting was employed by using Shirley and U2 Tougaard background. The total area percentages were computed by measuring the area under the respective curves. All data analyses were performed by using CasaXPS Software (Demo v.2.3.25) [116].

3.3 Cell Studies

3.3.1 Cell Culture and Differentiation

SH-SY5Y cells (ECACC, European Collection of Authenticated Cell Cultures, Catalogue No. 94030304) were maintained in culture medium composed of DMEM/F12 (1:1) with L-glutamine (Gibco), supplemented with 10% fetal bovine serum (FBS, Capricorn), and 1% penicillin/streptomycin (Hyclone) at 37°C and under 5% CO_2 in

a humidified atmosphere. The growth medium was changed every 3 days.

After reaching confluence, cells were harvested and seeded on substrates. For inducing neuronal differentiation, the growth medium was substituted with a differentiation medium consisting of standard medium with 1% FBS and 10 μM all trans-retinoic acid (ATRA) after 24 h of incubation. The medium was changed on alternate days and cells were incubated up to 11 days on samples. All experiments were performed with cells at passages between 11 and 13.

3.3.2 Cell Viability Assay

To assess the cell viability on the substrates, undifferentiated SH-SY5Y cells were plated on surfaces at a seeding density of $5x10^4$ cells/mL in a 24-well plate and evaluated with Alamar Blue assay after a culture period of 1, 4 and 7 days. On the specified days, the culture media was replaced with 10% alamarBlue™ (ThermoFisher Scientific) containing fresh medium and incubated for 4h at 37°C. After incubation period, 100 μL of aliquots were transferred in a 96 well plate and the absorbance values at 570 nm and 595 nm wavelengths were measured by using a microplate reader spectrophotometer (BIO-RAD iMark). For further measurements, the wells were washed with PBS and media were refreshed.

3.3.3 Immunocytochemistry and Neurite Length Analysis

For monitoring the neuronal differentiation and the neurite outgrowths of SH-SY5Y cells on substrates, cells were plated at a seeding density of $2.8x10^4$ cells/mL and differentiated for 11 days. At the end of this period, samples were fixed in 4% (w/v) paraformaldehyde (PFA) (Sigma) for 20 min, followed by permeabilization with Triton X-100 (0.1% v/v) for 5 min and washed with PBS after each step. After blocking with 1% bovine serum albumin (BSA, Biosera) in PBS containing 0.1% Tween 20 at 37°C for 30 min, anti-β3-tubulin (1:50, Santa Cruz, sc-80005) primary antibody

diluted in 1% BSA solution was incubated overnight at 4°C. Subsequently, samples were rinsed with PBS and incubated with Goat-anti mouse IgG H&L (1:100, Alexa Fluor 555, ab97035) secondary antibody for 2h at RT. Finally, the cell cytoskeleton and nuclei were stained using Alexa Fluor 488 conjugated phalloidin and 4',6-diamidino-2-phenylindole (DAPI) (Thermo Fisher Scientific) and the samples were visualized using fluorescence microscopy with a 20X objective lens (Leica DM IL). Each sample was randomly imaged at least three regions for quantitative analysis.

Neurite lengths were calculated by using NeuronJ semi-automated tracing plugin of ImageJ software. Prior to analysis, the distance was calibrated with a known scale of the image and the corresponding images were merged and stacked into RGB composites in FIJI (ImageJ) software. After converting images to 8-bit in TIF format, neurites that are longer than the cell body were quantified by tracing the processes beginning near the cell soma extending to the tip. The neurites were quantified by dividing the number of manually counted nuclei to the total neurite lengths. Neurites that are longer than the cell soma were selected for measurement. The values were normalized to PLL-P groups prior to statistical analysis.

3.4 Statistical Analysis

Statistical analysis was performed using GraphPad Prism 9.3.1 (GraphPad Software). Data were represented as mean ± standard deviation (SD) or median ± quartiles and mean ranks. Cell studies were conducted in biological replicates ($N = 3$). Two-way analysis of variance (ANOVA) with a Dunnett's post hoc multiple comparison test was carried out for comparison across two factors with more than one treatment. Neurite length measurements were analyzed via non-parametric Kruskal-Wallis test with Dunn's post-hoc multiple comparison test following the Shapiro-Wilk normality test. The results were considered as statistically significant where $* = p < 0.05$, $** = p < 0.01$, $*** = p < 0.001$, $**** = p < 0.0001$.

3.5 Results

3.5.1 Characterization of Surface Functionalization

Herein (Figure 3.2), the WCA of the gold surface measured 69.75 ± 3.3° in time after cleaning procedure. The adsorption of polyelectrolyte PLL molecules resulted in a more hydrophilic gold surface with a contact angle of 33.02 ± 3.3°. The WCA of the gold surface decreased to 50.83 ± 5.8° following the chemisorption of DSP molecules. The covalent attachment of PLL molecules via DSP crosslinker reduced the value to 35.43 ± 2.9° and showed similar hydrophilic character with PLL-P. Modification of DSP treated gold surfaces with N-Cadherin, NCAM and mixture (1:1) of these cell adhesion molecules exhibited values of 59.81 ± 3.1°, 62.38 ± 3.8°, and 66.46 ± 5°, respectively.

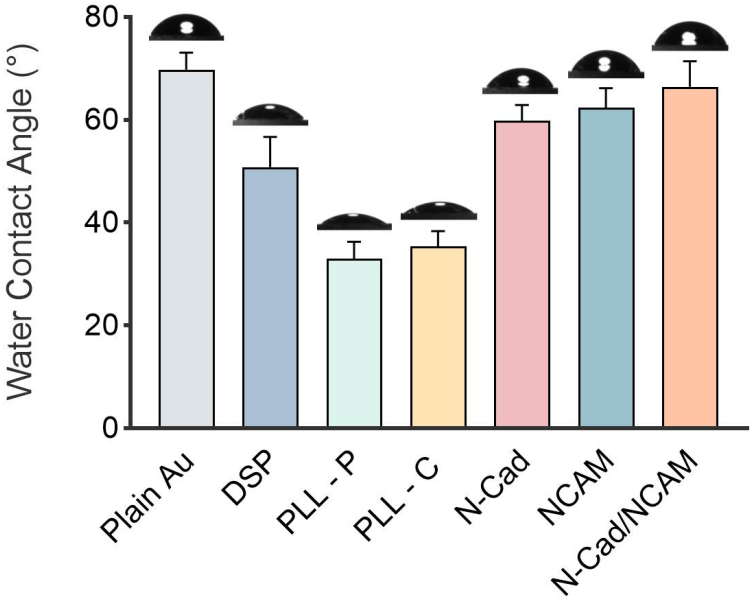

Figure 3.2 The result of water contact angle (WCA) measurements of gold surfaces before and after surface treatments ($n = 3$)

XPS was utilized to further characterize the variations in the chemical composition of substrates after each modification step, whereby the C1s high and N1s resolution signals are used to evidence the presence of functional groups of the correspondent molecules. The C1s deconvolution spectra of all the depositions (Figure 3.3 a) showed

characteristic aliphatic carbon peaks belonging to C-C/C-H bonds around 284.7-284.8 eV. The peak at 285.8 eV (Table 3.1) is attributed to C-S bond proving the chemisorption of DSP crosslinker with gold surface while the presence of C-O/C-N bonds in molecules were observed at 286.0 eV [117, 118]. The significant O=C-N/O=C-O peak at 288.9 eV is assigned to the functional groups of the NHS ester of DSP molecule [118–120]. Modification of surfaces with N-Cad, NCAM and N-Cad/NCAM mixture, additionally PLL molecule, showed peaks around 286.2 -286.6 eV which are correlated to C-S bond [119, 121]. Besides, the peaks in the range of 287.7-288.1 eV for those same molecules revealed O=C-N and O=C-O functional groups which are mainly attributed to amide and carboxylic acid coming from the peptide structure [122–125]. C-N/C-O peaks were also observed at 286, 286.3, 286.1, for N-Cadherin, NCAM and N-Cad/NCAM mixture respectively, while the C-N peak of PLL appeared at 285.7 eV [123, 125, 126]. PLL-P displayed amide and carboxylic acid groups at 287.9 eV which is similar to prior results. Additionally, the binding energies at 285.8 eV can be assigned to C-N species due to the absence of thiol interaction between the surface and the molecules, hereby C-S bonding.

Since the peak specific binding energies of each sample are close to each other, this may confound the comprehension of covalent modification to the surface. Although the peak specific percent total areas (%) may differ among the samples due to the variation in the chemical composition, an overall look at C-S bonding may enlighten the interaction of surface and DSP molecules. As can be seen from Table 3.1, the total percent areas belonging to C-S bonding of covalently modified samples are lower compared to DSP alone. This can be interpreted as the ratio of sulfur (S) compared to overall elements in covalently bonded molecules is below that of DSP, and the steric bulk affiliated with protein structure might have hindered the detection of these bonds. Since the PLL-P molecule does not have C-S bonding in its structure, it can be concluded that the binding energy around that value belongs to C-N species.

To further prove the modification of DSP molecules and proteins, the high resolution of N1s spectra was also examined. Two peaks appear at 399.4 eV and 401.7 eV in DSP molecules attributed to N-C=O or N-O-C species in NHS ester [118, 119, 127].

Table 3.1
Binding energies with corresponding assignments and total area percentages.

Species	Binding Energy (eV) & Total Area Percentages (%)						Assignment
	PLL-P	**DSP**	**PLL-C**	**N-Cad**	**NCAM**	**N-Cad/NCAM**	
C1s	284.7 (61.13%)	284.7 (53.32%)	284.8 (65.41%)	284.8 (62.18%)	284.8 (66.43%)	284.7 (65.82%)	Aliphatic carbon C-C/C-H
		285.8 (5.16%)	286.5 (3.06%)	286.6 (3.45%)	286.2 (1.46%)	286.3 (0.41%)	C-S
	285.8 (22.91%)		285.7 (12.22%)				C-N
		286.0 (21.69%)		286.0 (11.02%)	286.3 (20.93%)	286.1 (15.58%)	C-O/C-N
		288.9 (19.83%)					O=C-N/O=C-O NHS species
	287.9 (15.96 %)		287.8 (19.31%)	287.7 (23.36%)	288.1 (11.17%)	287.8 (18.19%)	O=C-N/O=C-O
N1s		399.4 (20.42%)					N-C=O NHS species
		401.7 (79.58%)					N-O-C NHS species
	399.9 (93.79%)		400.0 (84.38%)	399.8 (76.72%)	399.9 (89.84%)	399.8 (94.88%)	N-C=O (Amide)
	402.2 (6.21%)		401.9 (15.62%)	398.5 (23.28%)	402.5 (10.16%)	402.4 (5.12%)	NH_3^+/NH_2

The binding energies in the range of 399.8-400.0 eV (Figure 3.3 b) indicated the presence of amide bonds for the rest of the molecules [59, 126, 128–130]. Charged nitrogen (NH_3^+) signal from PLL amine groups was detected at 401.9 and 402.2 eV for PLL-C and PLL-P molecules, respectively [126, 131]. Amines (NH_2) in the form of primary, secondary, or tertiary structure and protonated amines (NH_3^+) that are components of proteins can be displayed at different binding energies. In this case, the binding energies related to these species for N-Cad, NCAM, N-Cad/NCAM molecules appeared at 398.5, 402.5, and 402.4 eV, respectively [121, 132].

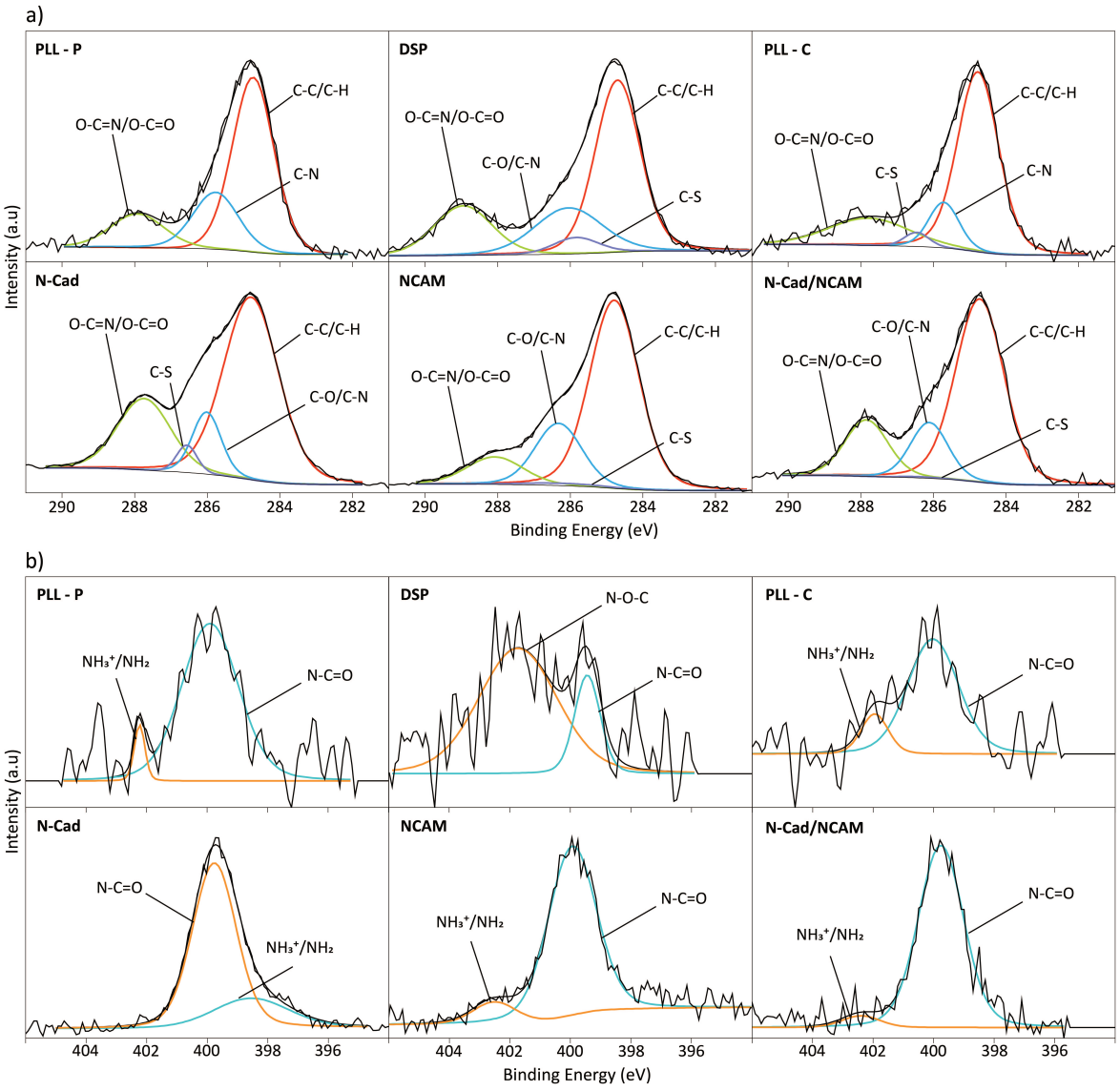

Figure 3.3 Deconvolutions of high-resolution a) C1s and b) N1s spectra of corresponding samples after treatments.

3.5.2 Cell Viability

The viability of SH-SY5Y cells was evaluated for plain and modified surface conditions. According to Figure 3.4, SH-SY5Y cells on all substrates remained metabolically active for 7 days. This result is overall indicating the non-toxic properties of all surfaces. On Day 1, the viability of cells on NCAM-containing surfaces outperform PLL-P surfaces, implicating a fast-acting proliferation effect by NCAM. The trend continues into Days 4 and 7 as both NCAM-containing surfaces consistently display highly significant boost in viability versus PLL-P. N-Cadherin on the other hand performs similarly to PLL-P on Day 1 but in subsequent days a delayed positive effect is observed on cell viability. These comparisons to PLL-P, which is the standard surface coating method in most in-vitro neural studies, also hold true when the groups are compared to PLL-C, available in the Dunnett's multiple comparison test given in Figure 3.5.

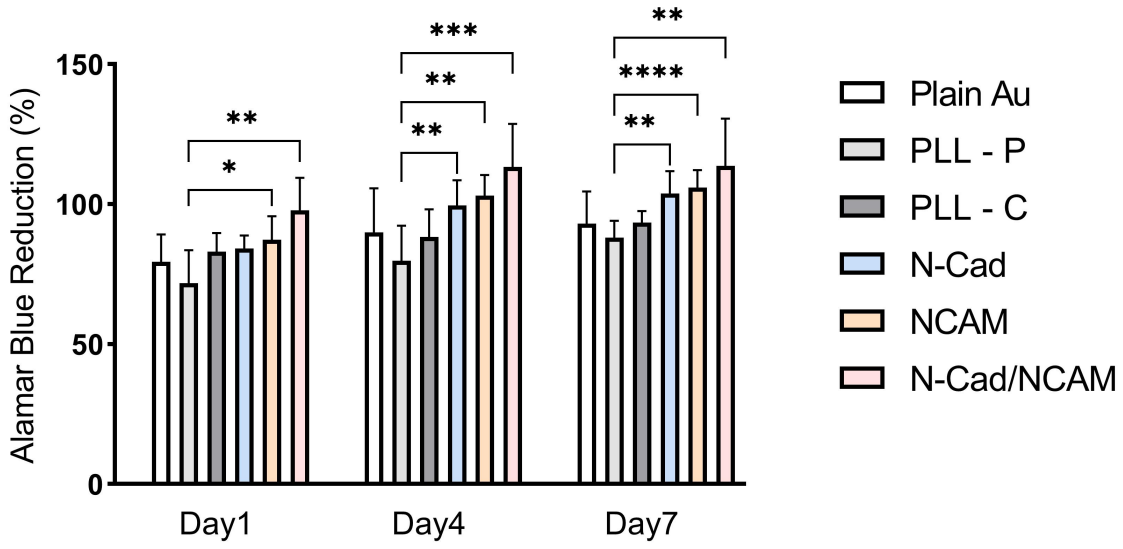

Figure 3.4 Reduced alamar blue (%) activity with relative SH-SY5Y viability on plain and treated surfaces over 7 days. Two-way ANOVA followed by Dunnett's multiple comparison test, comparing PLL-P vs. CAM interactions; *p $<$ 0.05, **p $<$ 0.01, ***p $<$ 0.001, ****p $<$ 0.0001. (n=3, N=3)

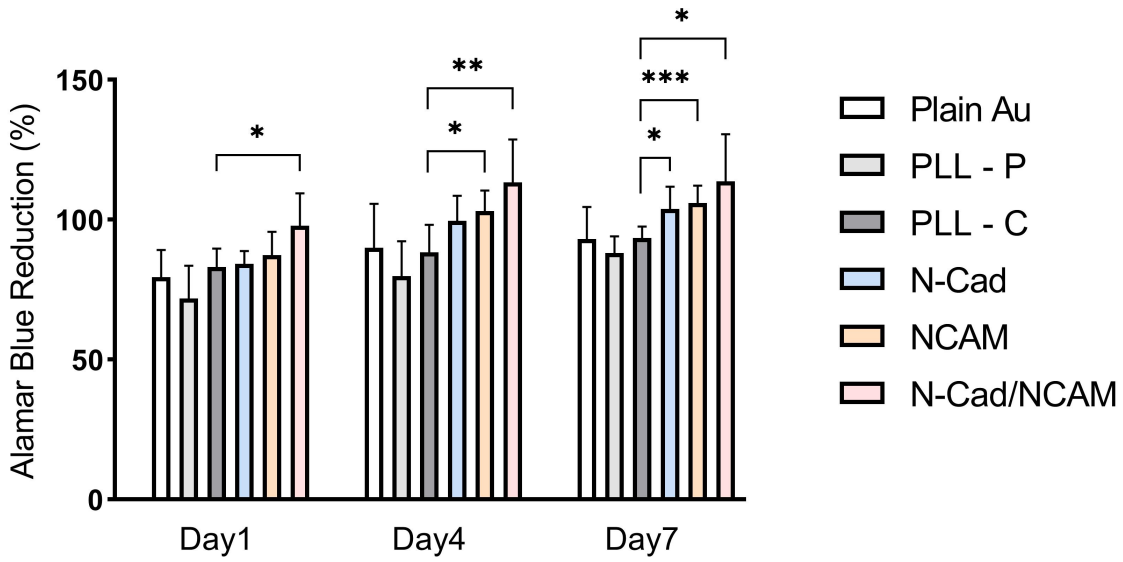

Figure 3.5 Alamar Blue Reduction (%). Two-way ANOVA followed by Dunnett's multiple comparison test, comparing PLL-C vs. CAM interactions; *p $<$ 0.05, **p $<$ 0.01, ***p $<$ 0.001, ****p $<$ 0.0001. (n=3, N=3)

3.5.3 Neurite Length Measurements

To analyze whether surface treatment with the defined cell adhesion molecules had an impact on neurite outgrowth besides biocompatibility, SH-SY5Y cells were treated with ATRA for 11 days to acquire fully differentiated neuronal phenotypes, and neurite lengths were measured. The change in the morphology of SH-SY5Y cells after the differentiation period was presented in Figure 3.6. The neurites that have distinct projections as opposed to undifferentiated cells were distinguished with a βIII tubulin neuronal marker, in combination with a phalloidin cytoskeleton dye (F-actin) and DAPI nuclear stain.

Figure 3.7 visually demonstrates that the surface functionalization, particularly in the case of NCAM-containing surfaces, resulted in a discernible increase in neurite outgrowth compared to the plain Au surfaces. To thoroughly understand whether the specified cell adhesion molecules have effect on neurite outgrowths, the mean ranks of the samples were compared against PLL, a well-known neuronal coating [133, 134].

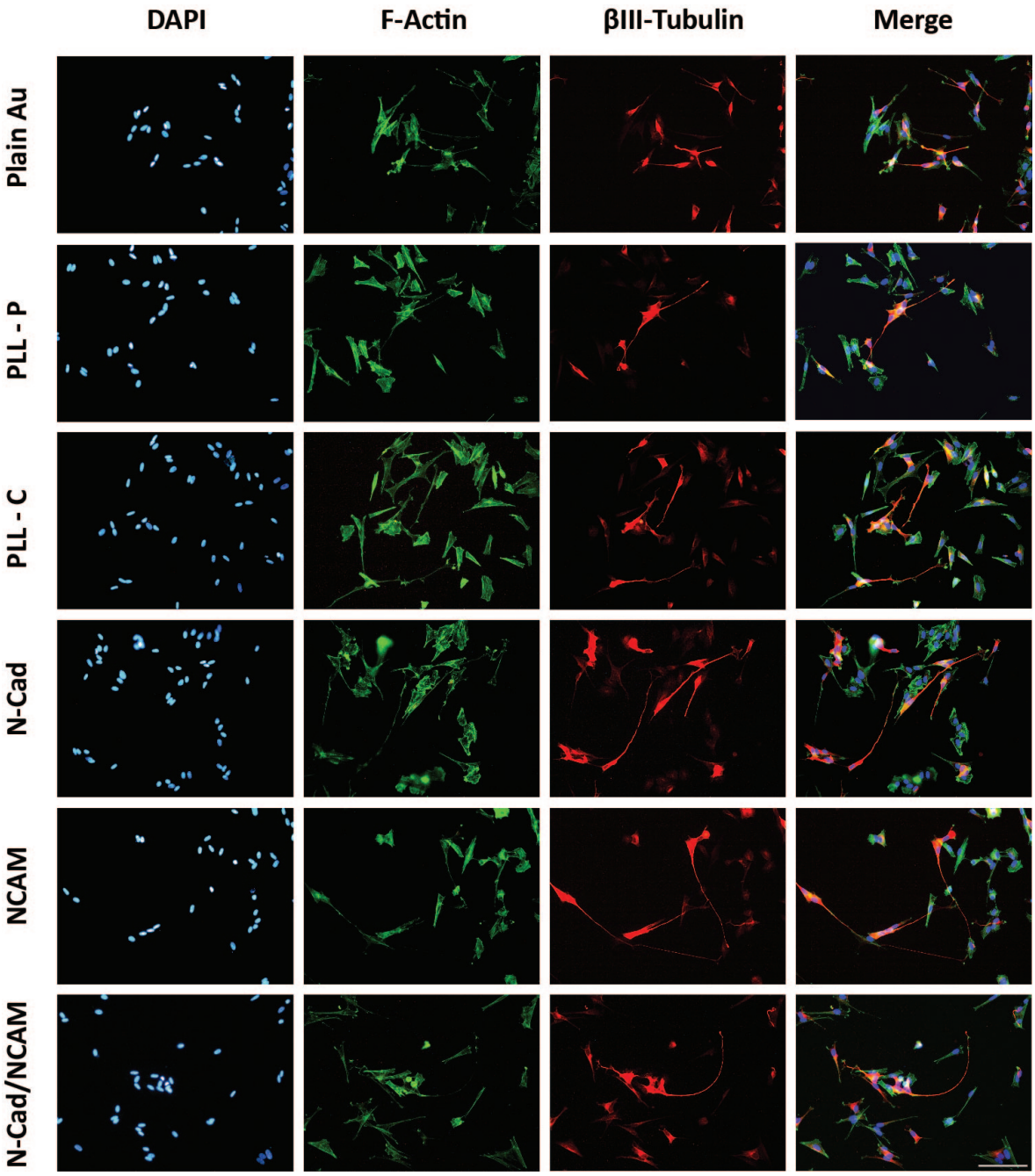

Figure 3.6 a) Immunofluorescent staining of SH-SY5Y cells differentiated 11 days on plain and treated surfaces. Cells were stained for βIII tubulin (red), F-actin (green), and DAPI (blue). Scale bar = 200 μm.

According to these results, NCAM and N-Cad/NCAM modified samples showed statistically significant differences compared to both PLL adsorbed (Figure 3.7) and PLL modified surfaces (Figure 3.8).

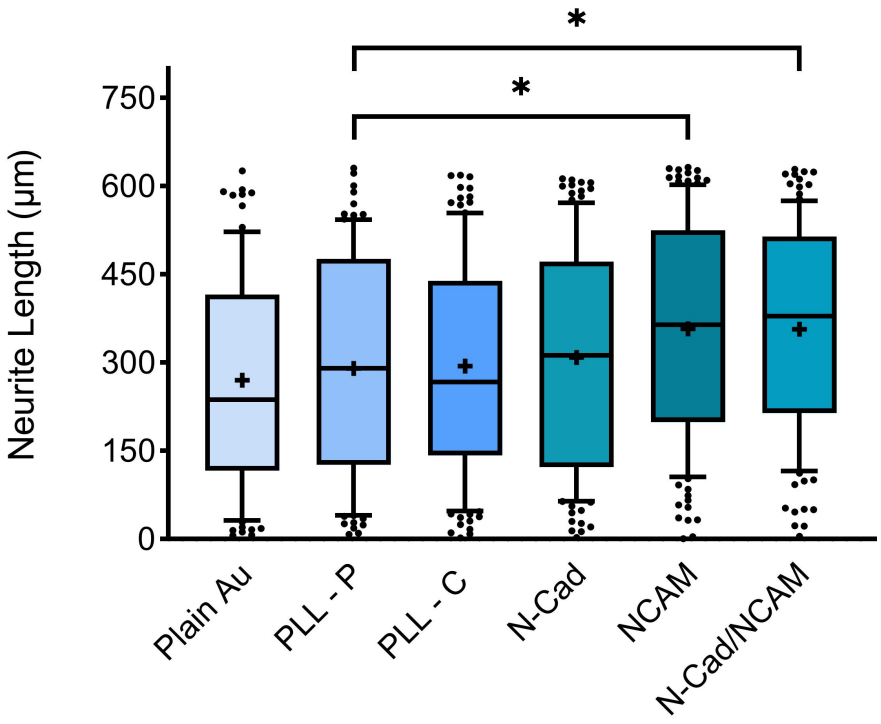

Figure 3.7 Quantification of neurite outgrowths of the samples. The line through the middle of the boxes shows the median. The dots represent 10-90 percentile range. The mean is shown as the "+" symbol inside the boxes. Data were analyzed via non-parametric Kruskal-Wallis test with Dunn's post-hoc multiple comparison test, comparing PLL-P vs. CAM interactions; *p $<$ 0.05, **p $<$ 0.01, ***p $<$ 0.001, ****p $<$ 0.0001. (n$\geq$ 3, N=3).

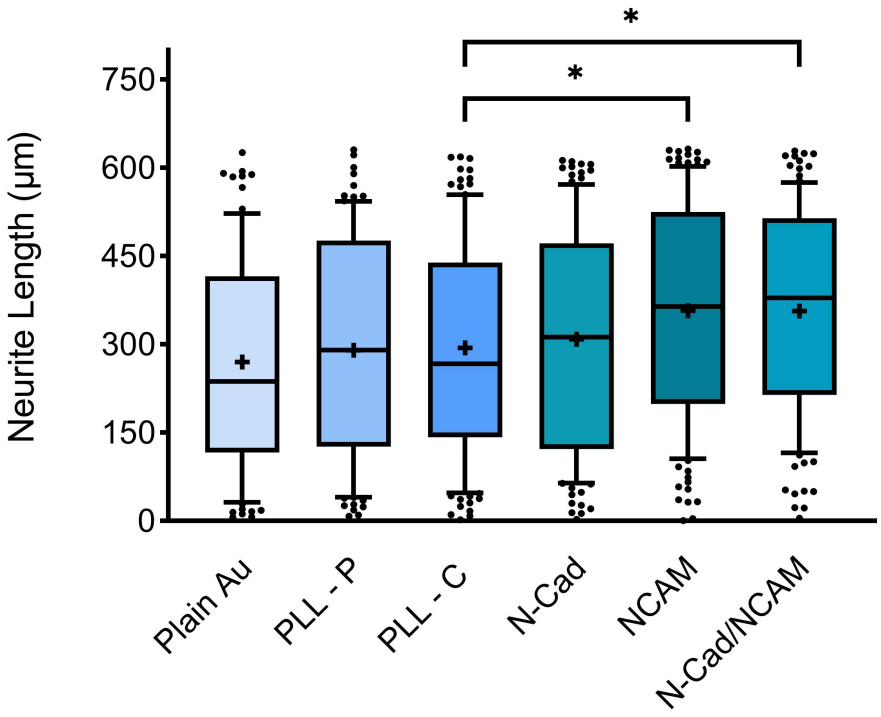

Figure 3.8 Quantification of neurite outgrowths of the samples with box plot. The line through the middle of the boxes shows the median. The dots represent 10-90 percentile range. The mean is shown as the "+" symbol inside the boxes. Data were analyzed via non-parametric Kruskal-Wallis test with Dunn's post-hoc multiple comparison test, comparing PLL-C vs. CAM interactions; *p $<$ 0.05, **p $<$ 0.01, ***p $<$ 0.001, ****p $<$ 0.0001. (n$\geq$ 3, N=3).

3.6 Discussion

The wettability of gold surfaces was evaluated by the water contact angle measurements. In the literature, pristine gold surfaces show different hydrophilic values starting from $\sim 0°$, and their exposure to air and organic contaminants increases their contact angle up to around 70° and even more over time [135–138]. The water contact angle of the gold surface closely approximated values around 70°, and this measurement, conducted sometime after the cleaning procedure, validated the values found in the literature. The decrease in contact angle observed after PLL adsorption and the covalent attachment of PLL molecules can be attributed primarily to the presence of polar side groups within PLL [122, 139, 140]. The decrease of WCA to 50.83 $\pm$ 5.8° following DSP molecule chemisorption indicated successful thiol-gold formation [141]. The modification of DSP-treated gold surfaces with N-Cadherin, NCAM, and a 1:1 mixture led to a change in wettability which was attributed to the elimination and

masking of polar NHS groups on the DSP-functionalized surface by the larger protein molecules.

The presence of characteristic aliphatic carbon peaks, representing C-C/C-H bonds, consistently observed around 284.7-284.8 eV in all adsorption and modification processes, strongly suggests the presence of these fundamental carbon bonds in the molecular structures involved. Furthermore, there was a notable increase in the total area percentages across all groups when compared to the DSP-only groups, providing clear evidence of the presence of proteins and the successful incorporation of these biomolecules onto surfaces. This increase in total area percentages underscores the effectiveness of the protein adsorption and modifications in the various groups. The C-S bond played a crucial role in confirming the chemisorption of the DSP group onto the gold surface, except in the case of the adsorbed PLL group, where it was not present [117, 118]. When examining the total percentage area values, it becomes evident that the C-S percentages experienced a reduction in covalently modified samples. This reduction may be attributed to the likelihood that the steric bulk associated with the protein's structure impeded the detection of these C-S bonds. In the instance of PLL-P molecules, the binding energy value of C-S undergoes a shift towards C-N. This shift can be attributed to the absence of C-S bonding within the PLL-P molecule's structure, leading to the inference that the binding energy around this value pertains to C-N species, which are also characterized by elevated percentages, primarily due to the existence of amine groups within the PLL molecule. This high percentage is similarly observed in the case of the PLL-C group, further corroborating the prevalence of C-N groups. The presence of significant peaks corresponding to O=C-N/O=C-O reactive sites in the NHS ester of the DSP molecule was further corroborated by the N1s high-resolution peaks. Surface modifications involving N-Cad, NCAM, a combination of N-Cad/NCAM, and PLL molecules unveiled the existence of O=C-N and O=C-O functional groups. These functional groups are mainly associated with amide and carboxylic acid components originating from the peptide structure. The N1s high-resolution spectra provided further evidence for the presence of amide bonds in the molecules. A consistent pattern emerged in the case of PLL-P, which exhibited amide and carboxylic acid groups clustered around the same peak value, mirroring the findings

from the other molecules. The confirmation of these groups was reinforced by the total area percentages. The signal from charged nitrogen ions (NH_3^+) stemming from the amine groups of PLL was identified at a similar binding energy value for both PLL-C and PLL-P molecules. It's noteworthy that amines (NH_2) in various structural forms, such as primary, secondary, or tertiary amines, as well as protonated amines (NH_3^+) that are integral components of proteins, can exhibit distinct binding energies. These different species were observed in the N1s spectra for N-Cad, NCAM, and N-Cad/NCAM molecules.

The results of the viability tests imply that, on the whole, all the surfaces tested exhibit non-toxic properties. Notably, surfaces containing NCAM demonstrated substantial cell viability at the conclusion of the experiment. These findings suggest that, compared to PLL coated surfaces compared to a simply positively charged surface presented by PLL coating, cell adhesion molecules have binding mechanisms including multi-protein complexes which also affect a wide spectrum of cell signaling mechanisms that may effectuate a more consistent environment by playing a direct or indirect role in cell viability [142]. N-Cadherin cascade is known to be associated with proliferation of mitotic cells which is in line with our findings [143]. NCAM on the other hand, was reported in the literature to be a major regulatory mechanism of neuronal differentiation where exposure of neural precursors to soluble NCAM results in the inhibition of proliferation and increased expression of neuronal markers [110]. Therefore, our data present a novel finding, suggesting that NCAM-mediated pathways are altered in proliferating SH-SY5Y cells and without ATRA-induced differentiation signals, the activation of NCAM receptors result in a rapid surge in proliferation. Considering that the SH-SY5Y is a human cancer-derived immortal cell line, this finding also carries implications for involvement of NCAM-regulated pathways in progression of neural tumors.

To assess whether the surface treatment involving specific cell adhesion molecules influenced neurite outgrowth, the change in the morphology of SH-SY5Y cells after the differentiation period was demonstrated with immunocytochemistry staining. Figure 3.7 provides a clear visual representation of the impact of surface functionalization on

neurite outgrowth, with a particularly significant increase observed in the case of surfaces containing NCAM, in contrast to the untreated Au surfaces. Our hypothesis is centered around the idea that the CAM modified surfaces will improve the integration of implants, thereby the biocompatibility while promoting the survival of nearby neurons. The formation of tissue encapsulation around the implant occurs as a result of a cascade of reactions initiated by the disruption of blood vessels during implantation. This disruption leads to the infiltration of blood components and inflammatory cells into the area, triggering the activation of glial cells. Ultimately, a noticeable reduction in neuronal density occurs in the immediate proximity of the implant site, commonly referred to as the "kill zone" [31, 34]. For the purpose of maintaining the prolonged functionality of chronically implanted electrodes, it is crucial to preserve neuronal survival and promote growth in close proximity to the implant site, typically within a range of 50-100 μm, since the recording electrodes need to establish close contact with the signaling neurons to capture single-unit activity.

Here, we chose N-Cadherin and NCAM due to their significant roles in various processes within the mature nervous system including the formation of synapses, axon guidance and fasciculation [109, 113, 144–146]. In various studies, researchers have been exploring the utilization of N-Cadherin as a surface coating to enhance neuron attachment and facilitate the extension of neurites [17, 18, 107, 147–149]. Paradies *et al.* revealed that purified NCAD90, when substrate-bound, maintains its biological function by facilitating cell adhesion and promoting neurite growth in a dose-dependent manner among chick embryo neural retina cells, suggesting that proteolysis of N-cadherin during embryonic retinal histogenesis serves as an endogenous regulatory mechanism that generates a unique and functional form of the protein, thus emphasizing the significance of NCAD90 in regulating cell adhesion and neurite growth during retinal development [147]. Additionally, Shi *et al.* presented a set of methods for obtaining surfaces with patterning multiple bioactive cues to understand how developing neurons integrate multiple biologically relevant signals and displayed control over neuron attachment and outgrowth by patterning L1 and N-cadherin proteins on surfaces. The findings of the study revealed that dendrites showed exclusive extension on N-cadherin patterns, whereas axons displayed a high level of selectivity towards

L1 patterns [149]. As previously mentioned, the studies regarding NCAM molecules have predominantly explored the effects of soluble or chimeric forms of NCAM, as well as the expression of NCAM on cells through transfection methods in the context of the neuron survival and regeneration. These investigations consistently demonstrate that the presence of NCAM, in a dose-dependent manner, effectively enhances neurite outgrowth [110–113, 150].

In comparison to the aforementioned findings, our study revealed that the maximum elongation occurred specifically when utilizing NCAM and N-Cad/NCAM functionalized surfaces. Upon reviewing the literature, it becomes apparent that cell behavior displays significant variability, primarily in response to the concentration or dose-dependent administration of molecules. This variability is further influenced by the specific types of CAMs and the manner in which they are presented [18, 147, 151–154]. As previously mentioned, Cherry *et al.* discovered that the use of a low concentration of N-Cad-Fc resulted in enhanced neuronal differentiation and the outgrowth of neurites. They applied human N-Cad-Fc at various concentrations ranging from 0.6875 to 5.5 μg/mL, either alone or in combination with 10 μg/mL of human L1-Fc. The researchers concluded that the density of N-Cad presented on the surface influenced the localization of cellular N-Cad, indicating its role in directing cellular response and function. This finding led them to suggest that low N-Cad-Fc substrates more accurately stimulate native N-Cad-mediated cell-cell contacts [18]. In our experiments, we observed similar effects concerning the impact of concentration. Our N-Cadherin modification also led to neurite outgrowth, although not to the same extent as observed with NCAM or the combination of N-Cad/NCAM. This disparity in outcomes may be attributed to the concentration utilized, which was 5 μg/mL, similar to the highest concentration mentioned in the article. Despite the fact that N-Cadherin has been reported to exhibit greater extensions compared to PLL in certain studies, we did not observe any statistically significant differences between the two groups, which may again be attributed to the concentration used [17, 155]. Furthermore, NCAM activation has long been linked to enhanced neurite extension length and induction of specific neural phenotypes, but it is worth noting that the same dose-dependent relationship applied to these molecules [90, 151, 156]. In the study conducted by Meiri *et*

al. the quantification of neurite outgrowth in cerebellar neurons was performed using different concentrations. The results demonstrated that 5 μg/mL of soluble NCAM-Fc exhibited the highest response compared to other concentrations [151]. Based on this finding, it is reasonable to assume that our NCAM modification may yield a similar outcome, as we are employing the same concentration of NCAM to the surfaces. Doherty *et al.* also conducted a study where they investigated the relationship between NCAM expression levels and neurite outgrowth by analyzing the morphology of cerebellar neurons cultured on 3T3 cells transfected with NCAM. They found that a minimum level of NCAM expression on 3T3 cells was necessary to initiate neurite outgrowth, and beyond this threshold, there was an exponential increase in neurite outgrowth with higher NCAM levels [150]. The outcomes achieved within this thesis, combined with the findings of the study, offer compelling evidence regarding the distinct effects of N-cadherin and N-CAM molecules on cellular dynamics, highlighting the significance of different concentrations in shaping the length of neurite outgrowth. These observations align with the existing literature on the subject, further strengthening our understanding of the topic. When considering the result of the combinations of molecules, one could speculate that the influence of NCAM may decrease as a result of the concentrations being halved for each molecule, regardless of the overall concentration. Nevertheless, an alternative viewpoint suggests that these mixtures create a state of equilibrium and collectively enhance neurite formation through a synergistic effect, especially when taking into account the notion that N-Cadherin tends to be more effective at lower concentrations [150].

This study introduces a novel finding by establishing a positive association between NCAM and N-Cad/NCAM combination coatings and the survival and outgrowth of neurons. It is crucial to recognize that the ability of neurite regeneration has the potential to minimize neuronal cell death, leading to improved biocompatibility of implants. Consequently, this capability can contribute to prolonging the lifespan and enhancing the effectiveness of the implant, thereby preventing a decline in the quality of signal measurements.

Prior investigations on NCAM coatings have either failed to yield significant

results or focused solely on neuronal adhesion. Furthermore, to the best of our knowledge, the synergistic effect of N-Cad/NCAM coatings has not been thoroughly examined in previous studies. Consequently, these findings offer great potential for the advancement of neurological devices by shedding light on the underlying mechanisms of CAM molecule interactions. This comprehension can unlock opportunities for pioneering modification techniques designed to enhance compatibility and effectiveness in the field.

3.6.1 Long-term Implications of Coatings and Future Prospects

As previously stated, the dynamic responses of cells at the electrode-tissue interface presents obstacles for the long-term clinical application of neural prosthetic devices. According to the research findings, there is a significant decrease in the functionality of electrodes starting from the first month of implantation [31, 157, 158]. Hence, researchers directed their efforts towards developing next generation implants with high-performance capabilities, aiming to enhance long-term biocompatibility. Currently, the application of scaffolds or surfaces for introducing CAMs has been limited to a small number of studies, particularly in terms of *in vivo* applications. However, there are studies indicating that these molecules have been effectively utilized up to 8 weeks of post-implantation without any adverse reactions or complications [11, 14, 159]. For example, Kolarcik *et al.* conducted a study examining acute and chronic responses over 1 or 4-week durations. The results showed notable findings with L1 immobilized electrodes. Specifically, a reduction in the rate of neuronal cell death was observed near the implant site in both the spinal cord (SC) and dorsal root ganglion (DRG) regions at both time points. Moreover, during the 4-week duration, there was evidence of a diminished "kill zone" in the SC regions, suggesting potential axonal regeneration to some extent [159]. In a prior study preceding this research, the modification of the same molecule on silicon probes was found to enhance neuronal density at acute (1 week) and as well as chronic (4 and 8 weeks) time intervals during *in vivo* studies [16]. The studies employed various approaches, including molecule adsorption or chemical modification, to achieve electrode modifications on the electrode surfaces and

they demonstrated that the stability of the modifications remained intact throughout the respective time periods. These investigations demonstrate the potential of cell adhesion molecules for long-term applications. Based on the findings, it can be concluded that our chemical modification method has also exhibited stability over a duration of approximately two weeks, as evidenced by the results of neurite extension. The DSP crosslinker is a well-established agent used in the process of modifying gold surfaces, employing a straightforward single-step covalent bond reaction. It is commonly applied for the attachment of antibodies, enzymes, and proteins onto gold surfaces, particularly in biosensor applications. Importantly, successful utilization of DSP modification has been demonstrated in both *in vitro* and *in vivo* studies, even over extended incubation periods, showcasing its effectiveness [160, 161]. Based on the aforementioned findings, it is evident that this modification method not only demonstrates a safe approach but also holds substantial potential for achieving successful outcomes in long-term research studies. Furthermore, the utilization of CAMs has been found to offer several advantages over traditional coatings such as laminin and PLL, specifically in terms of promoting long-term neuronal attachment, survival, and regeneration [17, 110, 147, 148, 155, 162–164]. In addition to these beneficial properties of CAM molecules, research studies have indicated their potential in inhibiting the formation of glial scars by reducing the activation of astrocytes and microglia or preventing the adhesion of these cells to the surfaces [19, 108, 113, 153, 165]. Hence, the utilization of CAM molecules can provide significant benefits by concurrently reducing glial scar formation and promoting neurite outgrowth. This attribute holds particular value in attenuating secondary damage induced by the release of inflammatory factors from these cells and extending the lifespan of the electrode. One challenge may arise due to the specificity of cell adhesion molecules in the context of surface modification and scaffold design intended for multiple cell types [96]. Hence, it is of importance to meticulously choose cell adhesion molecules that align with the desired cell types. To address this limitation, it may be necessary to implement supplementary strategies, such as incorporating multiple cell adhesion molecules or exploring alternative functionalization techniques. Furthermore, it is crucial to consider the interplay and synergistic effects among different CAMs. Our study, as well as other relevant research, provides compelling evidence of the positive outcomes associated with these interac-

tions [17, 18, 148, 150]. By precisely adjusting and identifying optimal concentration of CAM molecules, their collective efficacy can be maximized in improving the biocompatibility of implants. This is due to the fact that these CAM molecules indirectly intersect through shared pathways, such as FGFR and MAPK/ERK, further enhancing their overall impact [166, 167]. In addition to the combination of CAM molecules, the co-delivery of soluble and physical factors can be considered to enhance therapeutic outcomes. It should be emphasized that in cases of prolonged and severe inflammation, the aforementioned effects may not be fully effective. In such scenarios, a multi-faceted approach combining this system with supplementary methods, such as the incorporation of soft or dissolvable materials, the delivery of anti-inflammatory medications, or the inclusion of bioactive cues, may advance the process to a greater extent *[17, 150, 168–171]. For instance, the study by Doherty *et al.* demonstrated that combining nerve growth factor (NGF) with N-Cad can increase neurite outgrowth. Similarly, in the work by Collazos *et al.* the introduction of CAMs to conductive polymer PEDOT:PSS resulted in functional electrodes that maintained their electrical activity [17, 150, 171]. Xu *et al.* also utilized recombinant L1-Fc coated polyglycolic acid-chitosan conduit to promote guided regeneration and remyelination of injured optic nerves. Through the biodegradable nature of PGA-chitosan, *in vivo* experiments demonstrated substantial axonal regeneration, alongside the absorption of the conduit [172]. The potential of cell adhesion molecules extends beyond neural-electrode interfaces in neuromodulation and neuroprosthetic systems, as previously mentioned, showcasing their versatility in various applications. Their versatility for modification extends beyond neural-electrode interfaces in neuromodulation and neuroprosthetic systems to encompass neural tissue engineering applications, including the utilization in nerve guidance conduits or drug delivery particles [2, 173, 174]. Depending on the materials employed, these molecules can be applied through chemical crosslinking and biochemical conjugation techniques, especially when long-term functionality is required. Moreover, they can also be entrapped or immobilized within scaffolds, particularly hydrogels commonly used in neural tissue engineering applications [161, 174, 175]. Therefore, their adaptability to different systems and their potential for long-term applications make them a promising choice for advancing implant studies and neural tissue engineering. The integration of cell adhesion molecules with cutting-edge advancements is another crucial

aspect to consider in this context. Recent technological advancements have played a significant role in advancing the utilization of wireless equipment or fully-implantable devices [64, 176]. These advancements have introduced flexible and soft versions of electrodes that exhibit enhanced compatibility with neural tissue, while also minimizing the motion of the electrodes through size reduction or the creation of freely-floating designs [177–179]. However, despite these remarkable developments, challenges persist in areas such as material selection, electronic circuitry, and implantation techniques. Furthermore, despite advancements in neuromodulation technologies such as optogenetics, which eliminate the necessity of electrode insertion in specific applications, the majority of operations still rely on electrodes for direct acquisition of neural signals [180]. Thus, the integration of cell adhesion molecules remains crucial for current applications, serving as a hallmark in addressing these challenges. To summarize, the results of this part of thesis provide valuable insights that contribute to our understanding of the field of neural interfaces. However, to gain a deeper understanding of cell behavior and their long-term outcomes, it is imperative to diligently monitor and assess various types of neurons on NCAM and N-Cad/NCAM coatings in future studies. It is also crucial to comprehend how the CAMs utilized in this investigation contribute to reducing the formation of glial scars, as this knowledge can enhance the compatibility of devices. To attain a comprehensive understanding of their utilization and the impact on signal acquisition or transmission, further investigation is required to explore the combined influence of electrochemical properties and coatings. Moreover, conducting *in vivo* studies that encompass all the aforementioned aspects is necessary to assess the safety and long-term effects of these surfaces. Despite the limited existing studies demonstrating positive results of these molecules, there remains a significant gap in knowledge that needs to be further addressed and explored. Shedding light on this aspect is crucial for advancing our understanding in this field [17, 171].

4. Assessing Astrocyte Responses to Surface Modifications

This section of the thesis was conducted at the Institute for Technology-Inspired Regenerative Medicine (MERLN), with the cell studies specifically performed within the Department of Pharmacology-Toxicology of Maastricht University. The primary objective within this part of thesis was to investigate how glial fibrillary acidic protein (GFAP) levels of astrocytes change when exposed to surfaces coated with various molecules, including those modified with NCAM. It is noteworthy that the expression of GFAP increases in circumstances marked by cellular damage or inflammation, as also observed in the case of glial scar formation. This broader objective aimed to not only gain a deeper understanding of these responses but also to explore potential strategies for reducing the formation of glial scars around neural implants. According to existing literature and the study we have conducted and discussed previously, it is apparent that NCAM is a molecule recognized for its supportive role in neurons. Simultaneously, it has been observed to exert inhibitory effects on astrocytes [104–106]. With this objective in mind, a constrained study was carried out to evaluate the impact of NCAM on astrocytes. Additionally, Col-I modified surfaces were chosen as the negative control substrate due to recent findings suggesting a substantial increase in collagen content within the extracellular matrix (ECM) following brain injury, which contributes to formation of scar tissue.

Numerous studies employ Col-I not only for structural support but also to construct 3D models simulating glial scar formation in cell culture models. In this study, our assessment was intentionally directed towards 2D surfaces, with the primary aim of conducting a thorough comparison of the impacts stemming from coatings and modifications. This approach facilitated meticulous consideration of the precise concentrations of molecules utilized in the experiments.

Another objective was to induce a response in astrocytes through the application of Lipopolysaccharides sourced from Escherichia coli (LPS). This particular compound

constitutes a significant part of the cell wall in gram-negative bacteria. It possesses highly immunogenic properties, effectively boosting immune responses [181]. The objective was to attain a thorough comprehension of glial fibrillary acidic protein (GFAP) expression in C8D1A cells, with particular attention to its modulation by different concentrations of LPS.

4.1 Optimization of Surface Coatings and Cell Studies

4.1.1 Optimization of Surface Coatings

In this investigation, various surface coating methods were explored, including the modification of surfaces with the cell adhesion molecule, specifically NCAM, to assess their impact on astrocyte cells. A positive control (PDL or PDL/Laminin) was utilized to promote cell attachment and serve as a benchmark for comparing previously established cell behavior with NCAM modified surfaces. Simultaneously, a negative surface coating (Collagen-I) was employed to induce reactivity in astrocyte cells.

To achieve this objective, as an initial trial, glass coverslips were coated with poly-D-lysine (Sigma, P6407), a synthetic polymer with positive charge that promotes cell adhesion through interaction with the negatively charged ions on the cell membrane. This widely employed molecule in neural cell studies has been utilized to investigate cell responses to the modified surfaces [182–184].

With the objective in mind, glass coverslips (12 mm) were immersed in a 70% ethanol solution and placed on a rotator for 1h. After discarding the ethanol, the coverslips were rinsed with cell culture-grade water (HyClone, Cytiva). Subsequently, the coverslips were positioned on clean O-rings within a petri dish, and excess water was removed using a vacuum line. Poly-D-lysine (PDL), intended for use as the positive control, was prepared by diluting the stock solution (1 mg/ml) with cell culture-grade water to create a working solution (50 μg/mL). This prepared solution was gently added to the coverslips, with 150 μL applied to each, and then left to incubate at RT

for 1 h. Following solution removal by aspiration, the coverslips were transferred to non-treated 24-well plates. Subsequently, the coverslips were rinsed with sterile water and any excess water was aspirated.

The research also progressed by implementing PDL/Laminin and Collagen-I coating techniques. PDL/Laminin represents another established standard extensively utilized in studies involving neural applications [185, 186]. To achieve this objective, a PDL/Laminin solution was prepared by combining PDL and Laminin in a PBS solution at ratios of 1:100 and 1:50, respectively. This solution was applied to each coverslip (150 μL per coverslip) and left to incubate overnight.

A negative control utilizing a Col-I coating was also used to explore the possibility of stimulating astrocytes, inducing a shift from their ramified (resting) state to a reactive state [187–189]. As a result, it is expected to observe an increase in the expression of the glial fibrillary acidic (GFAP) protein, which is a key intermediate filament protein found in astrocytes. This expectation was based on the fact that the expression of these proteins typically rises in cases of cellular damage or inflammation. For this purpose, a working solution of collagen type I was prepared by diluting it in a 20 mM (0.02M) acetic acid solution at a 1:200 ratio, resulting in a final concentration of 50 μg/mL. Similarly, the working solutions were added to the coverslips and incubated for 2 h at 37°C. Throughout the preparation process, all solutions mentioned were maintained on ice.

Following the incubation periods, the solutions were removed, and the coverslips were initially transferred to non-treated 24-well plates and rinsed with PBS.

4.1.2 Preparation and Modification of Gold Surfaces

Au-coated 15 mm borosilicate float glass coverslips were cleaned according to the procedure outlined in section 3.1. To introduce N-hydroxysuccinimide (NHS) ester groups, the gold surfaces were immersed in a solution of 4 mg/mL DSP dissolved

in DMSO for a duration of 30 minutes at RT. After the DMSO and water rinsing procedure, the surfaces were placed on O-rings and underwent immediate covalent functionalization with NCAM (Sino Biological, 80399) for a duration of 2h at RT. This process was carried out using a total protein concentration of 5 μg/mL NCAM in phosphate buffered saline (PBS) (1X, pH 7.4). Following functionalization, the surfaces were washed with PBS and made ready for cell culture experiments. Cleaned uncoated surfaces were also reserved serving as plain (control) surfaces. To prepare the negative and positive control samples, the same procedure outlined in section 4.1.1 was employed. The cleaned gold surfaces, positioned on O-rings, were coated with a working solution of Poly-D-lysine (PDL)/Laminin and Col-I.

4.1.3 Cell Culture

The studies involved the use of C8-D1A [Astrocyte type I clone] cells which were generously provided by Prof Sebastien Foulquier to investigate astrocyte cell behavior on modified neural surfaces. C8-D1A cells, derived from mouse cerebellum, are employed in neuroscience research studies for their astrocytic properties [190–192].

C8-D1A cells were cultured in growth medium comprising DMEM high glucose supplemented with GlutaMAX, pyruvate, 10% heat-inactivated FBS, and 1% penicillin/streptomycin. The growth medium was renewed every 2-3 days. Upon reaching 70% confluency, the cells were trypsinized using 0.25% (w/v) trypsin-EDTA solution for 3 min and subsequently transferred to a 15 mL tube. After that, the cells were centrifuged at 125g for 5 min, and the supernatant was discarded. The cells were resuspended in 1 mL of complete medium for counting procedure. Cells within passage numbers 8-25 were utilized for these experiments.

For freezing the cells, the cells were subcultured. The medium was aspirated, and a 0.25% (w/v) trypsin-EDTA solution (3 mL for T75 flask) was introduced into the flask, followed by a 3 min incubation. Once the cells detached, 10 mL of complete growth medium was added, and the cells were gently pipetted into 15 mL tubes.

Following centrifugation at 125g for 5 min, the supernatant was removed. The cells were resuspended in 1 mL of freezing medium A, containing complete growth medium with 20% FBS, for each T75 flask. Subsequently, the cells were aliquoted into cryovials at 0.5 mL per vial, and 0.5 mL of freezing medium B, containing 10% DMSO, was gradually added drop by drop. The vials were labeled and placed in a freezing tube, kept at -80°C overnight, and then transferred to liquid nitrogen.

In all these experiments, cell seeding concentrations ranging from $2.2\text{x}10^4$ to $5\text{x}10^4$ cells/mL were used, depending on the specific application and surface area.

4.1.4 Optimization of LPS and Its Impact on Cellular Response

For this specific set of experiments, cells were introduced to 12 mm PDL/Laminin coated glass coverslips. Following a day from the initial cell seeding, the cells underwent treatment with both low and high concentrations of LPS (Sigma, L4391) for a duration of 24 h. Control wells without LPS treatment were set up, along with negative control cells for antibody staining. After conducting thorough literature research, the concentrations were established at 200 ng/mL for the low concentration and 1 μg/mL for the high concentration of LPS [190, 191].

4.1.5 Immunocytochemistry

For the assessment of astrocyte reactivity and proliferation in C8-D1A cells across various substrates, a 3-day culturing period was employed. At the conclusion of this period, a 4% working solution of formaldehyde was prepared by diluting a 37% formaldehyde stock solution (Sigma, 252549) in PBS. The samples were then fixed in this formaldehyde solution for 10 min at RT, followed by PBS rinse. Following fixation, permeabilization was carried out using Triton X-100 (0.1% v/v) (Merck, T8787) for 5 min. Subsequent to PBS wash, blocking was performed for 1h at RT using a solution composed of 5% bovine serum albumin (BSA) and 0.1% Tween 20 (Sigma-Aldrich,

P9416) in PBS. Subsequently, the samples were positioned on O-rings and treated with 150 μL of the primary antibody each, namely GFAP (Polyclonal Sheep IgG) (1:100) (RD Systems, AF2594). This step was executed utilizing a solution comprising a wash buffer, which was achieved by diluting the blocking buffer solution at a ratio of 5:1. This was followed by a 2h incubation at 37°C within a humidified chamber. Cells assigned to the negative control groups were subjected to incubation in a 1% BSA with 0.1% Tween 20 solution instead. After thorough buffer rinsing to eliminate unbound antibodies, the secondary antibody, Donkey anti-Sheep IgG (H+L) cross-adsorbed (1:250, Alexa Fluor™ 647) (Invitrogen, A21448), was applied in wash buffer and incubated under the same conditions. Finally, the cell cytoskeleton and nuclei were stained using Alexa Fluor 488 conjugated phalloidin (Invitrogen, A12379) and Hoechst 33342 (Invitrogen, H1399), respectively. Sample visualization was achieved using a fluorescent microscope (Nikon Eclipse Ti-E) with a 20X objective lens. To ensure the integrity of quantitative analysis, a minimum of three distinct regions within each of the five samples (n=5) was systematically selected and examined. Moreover, it is important to note that our study encompassed two independent biological replicates, further enhancing the validity of our findings.

The quantification analysis was executed through the utilization of ImageJ2, where a customized script was employed to facilitate the quantification of fluorescence intensity. Briefly, the code duplicates the phalloidin channel, applies thresholding to segment regions of interest, converts the thresholded image to a binary mask, creates a selection from the mask, and then measures various properties of the selected region. This process is repeated for GFAP channel, and the resulted mean values are stored. This code was designed to automate the analysis of fluorescence images. By automating the process, data analysis was streamlined, leading to consistent results. This approach facilitated the efficient quantification and comparison of fluorescence data across a multitude of images.

The same staining protocol was applied for the LPS experiments as well. Sample visualization was achieved using the same fluorescent microscope with a 20X objective lens. To maintain the reliability of the quantitative analysis, a minimum of six distinct

regions within each of the three samples (n=3) were systematically chosen and scrutinized. Quantification was conducted using ImageJ2, utilizing the same script as in the experiments mentioned above, with the sole modification being the adjustment of the threshold. Subsequent analyses were conducted using GraphPad Prism.

4.1.6 Statistical Analysis

The statistical analysis of the experiments was performed using GraphPad Prism 9.3.1. The results were analyzed via non-parametric Kruskal-Wallis test with Dunn's post-hoc multiple comparison test following the Shapiro-Wilk normality test. Data were represented as median ± quartiles supplemented by the mean. In the LPS groups, a one-way analysis of variance (ANOVA) was applied, followed by a Dunnett's post-hoc multiple comparison test for statistical analysis. The results were considered as statistically significant where $* = p < 0.05$, $** = p < 0.01$, $*** = p < 0.001$, $**** = p < 0.0001$.

4.2 Results

4.2.1 Refined Surface Coating Strategies and Cell Responses

In the presence of PDL coating, cell aggregation occurred, leading to suboptimal dispersion on glass coverslips when compared to conditions on TCP, which produced more favorable outcomes. Following the acquisition of these outcomes, the experiments were repeated to ascertain whether the challenge originated from the coating. Additionally, the samples were incubated once more at either RT or within a 37°C incubator for 1h. Nevertheless, consistent outcomes were achieved.

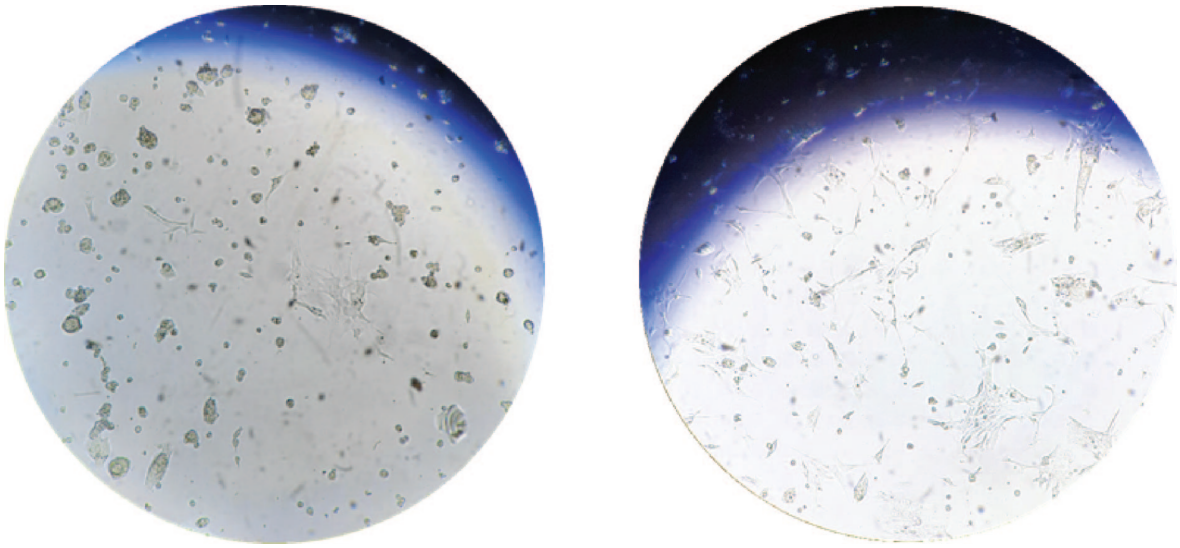

Figure 4.1 Bright-field images of C8D1A cells on PDL coated glass coverslips (left) and TCP surfaces (right). (The images were captured using a phone camera due to the absence of a camera system on the microscope.)

Cells adhered and proliferated on the surfaces coated with PDL/Laminin and Col-I. There were observed clumps on the surfaces coated with Col-I, alongside cells that adhered less uniformly. This raised concerns that Col-I might not be promoting effective cell spreading. However, following procedure optimization and adjustment of cell numbers, the Col-I method was successfully employed. The use of PDL/Laminin as a positive surface coating and Col-I as a negative surface coating was continued for the subsequent experiments.

4.2.2 Immunocytochemistry Results

The data obtained from gold surface experiments were assessed using median values as reference points, and mean values were additionally represented as white dots on the graph (Figure 4.2).

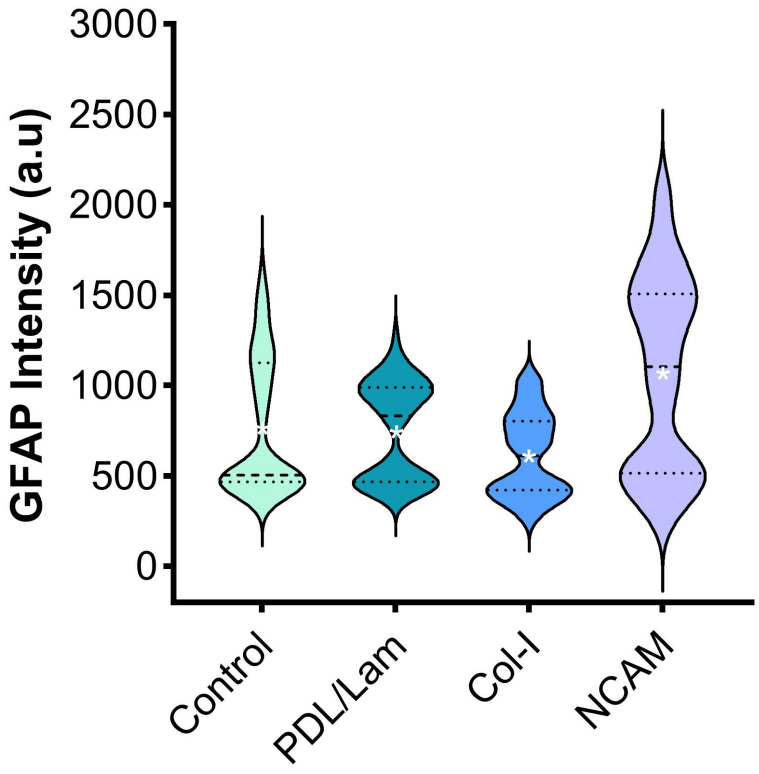

Figure 4.2 Quantification of GFAP intensity levels on unmodified and coated 2D gold surfaces. Data were analyzed via non-parametric Kruskal-Wallis test with Dunn's post-hoc multiple comparison test, comparing control vs. surface modifications; *p $<$ 0.05, **p $<$ 0.01, ***p $<$ 0.001, ****p $<$ 0.0001. (n=5, N=2).

There were no statistically significant differences observed when compared to the control surfaces. Contrary to our initial expectations, the mean GFAP intensity values on PDL/Lam surfaces were not significantly lower when compared to the plain gold surfaces. In terms of median values, PDL/Lam surfaces exhibited higher medians. Nevertheless, the intensity values on PDL/Lam coated surfaces demonstrated a more consistent distribution, with the median and mean values closely aligned. In contrast, GFAP intensity on plain gold surfaces exhibited variability, resulting in higher intensity values, even though the median was lower than PDL/Laminin.

On the contrary, Col-I produced unexpected results, showing a more desirable distribution pattern and lower intensity values. This contrasts with the initial hypothesis that Col-I had the potential to induce astrocyte reactions [187, 193]. Moving forward, the NCAM surfaces displayed a broader distribution of intensity values, along

with higher mean and median values that were closely aligned. This convergence of mean and median values might suggest a balanced distribution, implying that NCAM could potentially modulate astrocyte responses, either mitigating or provoking them.

In the LPS experiments, as illustrated in Figure 4.3, the greatest intensity was observed at a concentration of 1 μg/mL LPS. In this specific experiment, both LPS treatments demonstrated effectiveness, and a noticeable trend of increased GFAP protein expression in C8D1A cells was observed with rising LPS concentrations. However, statistically significant differences were only observed between the control group (without LPS) and the high concentration group (1 μg/mL).

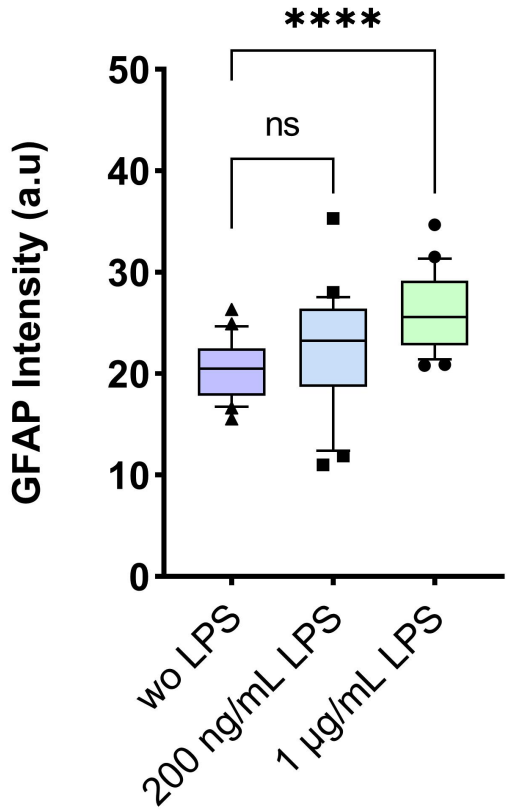

Figure 4.3 Effect of high concentration (1 μg/mL) and low concentration (200 ng/mL) of LPS on C8D1A cells cultured on glass coverslips. One-way analysis of variance (ANOVA) was applied, followed by a Dunnett's post-hoc multiple comparison test, comparing control (w.o LPS) vs. low and high concentration of LPS treatments; *p $<$ 0.05, **p $<$ 0.01, ***p $<$ 0.001, ****p $<$ 0.0001.

4.3 Discussion

During the surface coating experiments, it was noted that PDL-coated surfaces formed clumps at the surface, and proper dispersion did not occur. This phenomenon of clustering has also been observed and documented in the research conducted by Stil *et al.*, revealing that the adsorption of PDL, particularly on glass surfaces, tends to result in the formation of cell clusters after a few days [19]. Following successful optimization with PDL/Laminin and Col-I coatings, it was determined to proceed with these molecules for the subsequent experiments. In the experiment involving the surface modification of gold, it was noted that NCAM modified surfaces displayed a broader range of GFAP intensity distribution when compared to the other surface treatments. Despite the findings in the literature, it is not possible to definitively conclude a specific assumption regarding the inhibitory effect of the NCAM molecule on astrocyte reactivity. However, it can be postulated that NCAM may have a dual effect, meaning it might either decrease or increase the expression of GFAP, depending on specific conditions or factors. Furthermore, these effects may vary from cell to cell. Regarding Col-I, an intriguing contrary effect has been observed compared to the findings in the literature. In many studies, it has been noted that the prevention of glial scar formation can be achieved by blocking the interaction between reactive astrocytes and type I collagen [194, 195]. Hence, it can be suggested that in the presence of Col-I, astrocytes should transition to a reactive state and express GFAP more prominently than in their ramified state. However, this did not occur in this particular case. Furthermore, in prior studies, it was noted that primary astrocytes obtained from rats and cultured in appropriate Col-I concentrations maintained a relatively less activated or "naive" phenotype in contrast to those cultured in a 2D environment [196, 197]. Hence, it can be concluded that the role of Col-I remains a subject of debate, and the response of astrocytes to Col-I may also vary depending on factors such as concentration, cell type, and other variables. In terms of cell type, specifically for this particular cell type, while the study conducted by Hawkins *et al.* suggests that C8D1A cells in Col-I gel display reduced levels of GFAP compared to their 2D counterparts, there is a dearth of equivalent data to support this assertion [193]. Moreover, based on our current understanding, no other research is accessible to either support or challenge the influence

of GFAP expression on C8D1A cells. Considering the potential for varying responses among different cell lines to external stimuli, it is conceivable that the C8D1A cell line might demonstrate a distinct reaction to Col-I within a 2D environment. This specific response pattern could potentially deviate from the broader trends observed in other astrocyte cell lines. This phenomenon underscores the intricate nature of cellular behavior and the significance of acknowledging cell line-specific nuances to accurately interpret experimental outcomes. As a reference for future studies, we also examined the impact of varying LPS concentrations on GFAP intensities for this specific cell type. The LPS experiments demonstrated that a concentration of 1 μg/ml of the molecule could effectively prompt astrocytes to shift from a ramified to a reactive state. This transition was evident in the GFAP intensity results, showing statistically significant differences when compared to control surfaces. Conversely, a concentration of 200 ng/ml was found to be insufficient to induce this transition and did not exhibit statistically significant differences from the control surfaces. Nevertheless, it is advisable to conduct further optimization to ensure the stability of the molecule's effect in future research endeavors.

5. CONCLUSION

In the initial segment of this thesis, our findings demonstrate that cell adhesion molecule modified surfaces, particularly NCAM and N-Cad/NCAM modified, have the potential to be used in the fabrication of neuroprosthetic devices in respect to their biocompatible and neurite extension features. Moreover, DSP facilitated molecule modification provides feasible functionality as well as shortening the modification time. With this method, covalent modification of PLL was also indirectly compared with adsorbed PLL and there were no significant differences found between two groups. Therefore, either method can be used interchangeably, however the effect on long-term cell culture stability should be kept in mind. Additionally, a combination of the cell adhesion molecules was involved in this study to explore the synergistic effect of the molecules. While there is evident interaction with the cells, further optimization of this combination is necessary by investigating the effects of varying concentrations of each molecule.

In the subsequent section of this thesis, we explored the effects of various surface coatings on astrocyte behavior and GFAP expression, with a particular focus on understanding the mechanisms underlying glial scar formation and seeking potential solutions to mitigate it. NCAM-modified surfaces revealed a broader range of GFAP intensity distribution, which challenged previously held assumptions regarding astrocyte reactivity. Furthermore, taking into account the divergent outcomes we observed, it becomes evident that the function of Col-I is multifaceted, accentuating its intricate and complex impact on astrocyte behavior. Additionally, the study emphasizes the importance of adopting a detailed and context-dependent approach when investigating astrocyte behavior and the involvement of surface coatings in diverse experimental scenarios. LPS experiments also shed light on the potential for astrocyte transition at specific concentrations.

In summary, the modification of cell adhesion molecules holds promise for en-

hancing neuroprostheses and uncovering valuable insights in pursuit of new pathways to improve interfaces. These modifications may enhance neuronal survival and promote biocompatibility. However, our research underscores the intricate nature of interactions between surfaces and astrocytes, emphasizing the need for a thorough exploration to gain a comprehensive understanding of neurobiology and tissue engineering.

REFERENCES

1. Szostak, K. M., L. Grand, and T. G. Constandinou, "Neural Interfaces for Intracortical Recording: Requirements, Fabrication Methods, and Characteristics," *Frontiers in Neuroscience*, Vol. 11, 2017.

2. Campbell, A., and C. Wu, "Chronically Implanted Intracranial Electrodes: Tissue Reaction and Electrical Changes," *Micromachines*, Vol. 9, p. 430, Aug. 2018.

3. Im, C., and J.-M. Seo, "A review of electrodes for the electrical brain signal recording," *Biomedical Engineering Letters*, Vol. 6, pp. 104–112, Aug. 2016.

4. Kansaku, K., "Neuroprosthetics in systems neuroscience and medicine," *Scientific Reports*, Vol. 11, p. 5404, Mar. 2021.

5. Kelly, A., L. Ballerini, M. Lowery, and M. Biggs, "7.32 Engineering the Neural Interface," in *Comprehensive Biomaterials II*, pp. 642–660, Elsevier, 2017.

6. Aregueta-Robles, U. A., A. J. Woolley, L. A. Poole-Warren, N. H. Lovell, and R. A. Green, "Organic electrode coatings for next-generation neural interfaces," *Frontiers in Neuroengineering*, Vol. 7, 2014.

7. Hong, G., and C. M. Lieber, "Novel electrode technologies for neural recordings," *Nature Reviews Neuroscience*, Vol. 20, pp. 330–345, June 2019.

8. Foremny, K., W. Konerding, A. Behrens, P. Baumhoff, U. Froriep, A. Kral, and T. Doll, "Carbon-Nanotube-Coated Surface Electrodes for Cortical Recordings In Vivo," *Nanomaterials*, Vol. 11, p. 1029, Apr. 2021.

9. Kim, G., K. Kim, E. Lee, T. An, W. Choi, G. Lim, and J. Shin, "Recent Progress on Microelectrodes in Neural Interfaces," *Materials*, Vol. 11, p. 1995, Oct. 2018.

10. Lecomte, A., E. Descamps, and C. Bergaud, "A review on mechanical considerations for chronically-implanted neural probes," *Journal of Neural Engineering*, Vol. 15, p. 031001, June 2018.

11. Golabchi, A., K. M. Woeppel, X. Li, C. F. Lagenaur, and X. T. Cui, "Neuroadhesive protein coating improves the chronic performance of neuroelectronics in mouse brain," *Biosensors and Bioelectronics*, Vol. 155, p. 112096, May 2020.

12. Zhong, Y., and R. V. Bellamkonda, "Dexamethasone Coated Neural Probes Elicit Attenuated Inflammatory Response and Neuronal Loss Compared to Uncoated Neural Probes," *Brain research*, Vol. 1148, pp. 15–27, May 2007.

13. Klaver, C. L., and M. R. Caplan, "Bioactive surface for neural electrodes: Decreasing astrocyte proliferation via transforming growth factor-β1," *Journal of Biomedical Materials Research Part A*, Vol. 81A, no. 4, pp. 1011–1016, 2007.

14. Azemi, E., C. F. Lagenaur, and X. T. Cui, "The surface immobilization of the neural adhesion molecule L1 on neural probes and its effect on neuronal density and gliosis at the probe/tissue interface," *Biomaterials*, Vol. 32, pp. 681–692, Jan. 2011.

15. Webb, K., E. Budko, T. J. Neuberger, S. Chen, M. Schachner, and P. A. Tresco, "Substrate-bound human recombinant L1 selectively promotes neuronal attachment and outgrowth in the presence of astrocytes and fibroblasts," *Biomaterials*, Vol. 22, pp. 1017–1028, May 2001.

16. Azemi, E., W. R. Stauffer, M. S. Gostock, C. F. Lagenaur, and X. T. Cui, "Surface immobilization of neural adhesion molecule L1 for improving the biocompatibility of chronic neural probes: In vitro characterization," *Acta Biomaterialia*, Vol. 4, pp. 1208–1217, Sept. 2008.

17. Collazos-Castro, J. E., G. R. HernÃ¡ndez-Labrado, J. L. Polo, and C. GarcÃa-Rama, "N-Cadherin- and L1-functionalised conducting polymers for synergistic stimulation and guidance of neural cell growth," *Biomaterials*, Vol. 34, pp. 3603–3617, May 2013.

18. Cherry, J. F., N. K. Bennett, M. Schachner, and P. V. Moghe, "Engineered N-cadherin and L1 biomimetic substrates concertedly promote neuronal differentiation, neurite extension and neuroprotection of human neural stem cells," *Acta Biomaterialia*, Vol. 10, pp. 4113–4126, Oct. 2014.

19. Eles, J. R., A. L. Vazquez, N. R. Snyder, C. Lagenaur, M. C. Murphy, T. D. Kozai, and X. T. Cui, "Neuroadhesive L1 coating attenuates acute microglial attachment to neural electrodes as revealed by live two-photon microscopy," *Biomaterials*, Vol. 113, pp. 279–292, Jan. 2017.

20. Seidenfaden, R., A. Krauter, and H. Hildebrandt, "The neural cell adhesion molecule NCAM regulates neuritogenesis by multiple mechanisms of interaction," *Neurochemistry International*, Vol. 49, pp. 1–11, July 2006.

21. Bavishi, S., J. Rosenthal, and M. Bockbrader, "Chapter 17 - Neuroprosthetics," in *Rehabilitation After Traumatic Brain Injury* (Eapen, B. C., and D. X. Cifu, eds.), pp. 241–253, Elsevier, Jan. 2019.

22. Gupta, A., N. Vardalakis, and F. B. Wagner, "Neuroprosthetics: from sensorimotor to cognitive disorders," *Communications Biology*, Vol. 6, pp. 1–17, Jan. 2023.

23. Segal, M., "58 - Neuromodulation and neuroprosthetics," in *Brain Injury Medicine* (Eapen, B. C., and D. X. Cifu, eds.), pp. 357–360.e2, St. Louis (MO): Elsevier, Jan. 2021.

24. Sakas, D. E., I. G. Panourias, B. A. Simpson, and E. S. Krames, "An introduction to operative neuromodulation and functional neuroprosthetics, the new frontiers of clinical neuroscience and biotechnology," in *Operative Neuromodulation*, Vol. 97/1, pp. 3–10, Springer Vienna, 2006.

25. Iida, K., and H. Otsubo, "Stereoelectroencephalography: Indication and Efficacy," *Neurologia Medico-Chirurgica*, Vol. 57, pp. 375–385, Aug. 2017.

26. Fariba, K. A., and V. Gupta, "Deep Brain Stimulation," in *StatPearls*, Treasure Island (FL): StatPearls Publishing, 2023.

27. Ramos-Fresnedo, A., C. Perez-Vega, R. A. Domingo, W. P. Cheshire, E. H. Middlebrooks, and S. S. Grewal, "Motor Cortex Stimulation for Pain: A Narrative Review of Indications, Techniques, and Outcomes," *Neuromodulation: Technology at the Neural Interface*, Vol. 25, pp. 211–221, Feb. 2022.

28. Kumar, K., C. Toth, and R. K. Nath, "Spinal cord stimulation for chronic pain in peripheral neuropathy," *Surgical Neurology*, Vol. 46, pp. 363–369, Oct. 1996.

29. Shih, J. J., D. J. Krusienski, and J. R. Wolpaw, "Brain-Computer Interfaces in Medicine," *Mayo Clinic Proceedings*, Vol. 87, pp. 268–279, Mar. 2012.

30. Zhang, M., Z. Tang, X. Liu, and J. Van der Spiegel, "Electronic neural interfaces," *Nature Electronics*, Vol. 3, pp. 191–200, Apr. 2020.

31. Kozai, T. D. Y., A. S. Jaquins-Gerstl, A. L. Vazquez, A. C. Michael, and X. T. Cui, "Brain Tissue Responses to Neural Implants Impact Signal Sensitivity and Intervention Strategies," *ACS Chemical Neuroscience*, Vol. 6, pp. 48–67, Jan. 2015.

32. Oakes, R. S., M. D. Polei, J. L. Skousen, and P. A. Tresco, "An astrocyte derived extracellular matrix coating reduces astrogliosis surrounding chronically implanted microelectrode arrays in rat cortex," *Biomaterials*, Vol. 154, pp. 1–11, Feb. 2018.

33. Groothuis, J., N. F. Ramsey, G. M. J. Ramakers, and G. van der Plasse, "Physiological Challenges for Intracortical Electrodes," *Brain Stimulation*, Vol. 7, pp. 1–6, Jan. 2014.

34. Salatino, J. W., K. A. Ludwig, T. D. Y. Kozai, and E. K. Purcell, "Glial responses to implanted electrodes in the brain," *Nature Biomedical Engineering*, Vol. 1, pp. 862–877, Nov. 2017.

35. Gulino, M., D. Kim, S. Panè, S. D. Santos, and A. P. Pêgo, "Tissue Response to Neural Implants: The Use of Model Systems Toward New Design Solutions of Implantable Microelectrodes," *Frontiers in Neuroscience*, Vol. 13, p. 689, July 2019.

36. Nash, B., K. Ioannidou, and S. C. Barnett, "Astrocyte phenotypes and their relationship to myelination: Astrocyte phenotypes and myelination," *Journal of Anatomy*, Vol. 219, pp. 44–52, July 2011.

37. Vallejo-Giraldo, C., A. Kelly, and M. J. P. Biggs, "Biofunctionalisation of electrically conducting polymers," *Drug Discovery Today*, Vol. 19, pp. 88–94, Jan. 2014.

38. Sofroniew, M. V., and H. V. Vinters, "Astrocytes: biology and pathology," *Acta Neuropathologica*, Vol. 119, no. 1, pp. 7–35, 2010.

39. Rocha, D. N., J. P. Ferraz-Nogueira, C. C. Barrias, J. B. Relvas, and A. P. PÃªgo, "Extracellular environment contribution to astrogliosisâlessons learned from a tissue engineered 3D model of the glial scar," *Frontiers in Cellular Neuroscience*, Vol. 9, Sept. 2015.

40. Wu, V. W., and J. P. Schwartz, "Cell culture models for reactive gliosis: New perspectives," *Journal of Neuroscience Research*, Vol. 51, no. 6, pp. 675–681, 1998.

41. Wellman, S. M., L. Li, Y. Yaxiaer, I. McNamara, and T. D. Y. Kozai, "Revealing Spatial and Temporal Patterns of Cell Death, Glial Proliferation, and Blood-Brain Barrier Dysfunction Around Implanted Intracortical Neural Interfaces," *Frontiers in Neuroscience*, Vol. 13, 2019.

42. Edell, D., V. Toi, V. McNeil, and L. Clark, "Factors influencing the biocompatibility of insertable silicon microshafts in cerebral cortex," *IEEE Transactions on Biomedical Engineering*, Vol. 39, pp. 635–643, June 1992.

43. Adewole, D. O., M. D. Serruya, J. P. Harris, J. C. Burrell, D. Petrov, H. I. Chen, J. A. Wolf, and D. K. Cullen, "The Evolution of Neuroprosthetic Interfaces," *Critical reviews in biomedical engineering*, Vol. 44, no. 1-2, pp. 123–152, 2016.

44. Hong, G., R. D. Viveros, T. J. Zwang, X. Yang, and C. M. Lieber, "Tissue-like Neural Probes for Understanding and Modulating the Brain," *Biochemistry*, Vol. 57, pp. 3995–4004, July 2018.

45. Yang, W., Y. Gong, and W. Li, "A Review: Electrode and Packaging Materials for Neurophysiology Recording Implants," *Frontiers in Bioengineering and Biotechnology*, Vol. 8, 2021.

46. Cheung, K. C., "Implantable microscale neural interfaces," *Biomedical Microdevices*, Vol. 9, pp. 923–938, Dec. 2007.

47. Zeng, Q., and Z. Huang, "Challenges and Opportunities of Implantable Neural Interfaces: From Material, Electrochemical and Biological Perspectives," *Advanced Functional Materials*, Vol. 33, no. 32, p. 2301223, 2023.

48. Jules, A., "Fabrication of semiconductor devices," Mar. 1964.

49. Rousche, P. J., and R. A. Normann, "Chronic recording capability of the Utah Intracortical Electrode Array in cat sensory cortex," *Journal of Neuroscience Methods*, Vol. 82, pp. 1–15, July 1998.

50. Gwon, T. M., C. Kim, S. Shin, J. H. Park, J. H. Kim, and S. J. Kim, "Liquid crystal polymer (LCP)-based neural prosthetic devices," *Biomedical Engineering Letters*, Vol. 6, pp. 148–163, Aug. 2016.

51. Wester, B. A., R. H. Lee, and M. C. LaPlaca, "Development and characterization of in vivo flexible electrodes compatible with large tissue displacements," *Journal of Neural Engineering*, Vol. 6, p. 024002, Mar. 2009.

52. Altuna, A., E. Bellistri, E. Cid, P. Aivar, B. Gal, J. Berganzo, G. Gabriel, A. GuimerÃ , R. Villa, L. J. FernÃ¡ndez, and L. M. d. l. Prida, "SU-8 based microprobes for simultaneous neural depth recording and drug delivery in the brain," *Lab on a Chip*, Vol. 13, pp. 1422–1430, Mar. 2013.

53. Jorfi, M., J. L. Skousen, C. Weder, and J. R. Capadona, "Progress towards biocompatible intracortical microelectrodes for neural interfacing applications," *Journal of Neural Engineering*, Vol. 12, p. 011001, Dec. 2014.

54. Yin, P., Y. Liu, L. Xiao, and C. Zhang, "Advanced Metallic and Polymeric Coatings for Neural Interfacing: Structures, Properties and Tissue Responses," *Polymers*, Vol. 13, p. 2834, Jan. 2021.

55. Wu, N., S. Wan, S. Su, H. Huang, G. Dou, and L. Sun, "Electrode materials for brainâmachine interface: A review," *InfoMat*, Vol. 3, no. 11, pp. 1174–1194, 2021.

56. Fattahi, P., G. Yang, G. Kim, and M. R. Abidian, "A Review of Organic and Inorganic Biomaterials for Neural Interfaces," *Advanced materials (Deerfield Beach, Fla.)*, Vol. 26, pp. 1846–1885, Mar. 2014.

57. Saddow, S. E., C. L. Frewin, F. A. Cespedes, M. Gazziro, E. Bernadin, and S. Thomas, "SiC for Biomedical Applications," *Materials Science Forum*, Vol. 858, pp. 1010–1014, 2016.

58. Moxon, K., S. Leiser, G. Gerhardt, K. Barbee, and J. Chapin, "Ceramic-based multisite electrode arrays for chronic single-neuron recording," *IEEE Transactions on Biomedical Engineering*, Vol. 51, pp. 647–656, Apr. 2004.

59. Cho, Y., and A. Ivanisevic, "TAT Peptide Immobilization on Gold Surfaces: A Comparison Study with a Thiolated Peptide and Alkylthiols Using AFM, XPS, and FT-IRRAS," *The Journal of Physical Chemistry B*, Vol. 109, pp. 6225–6232, Apr. 2005.

60. Sohal, H. S., A. Jackson, R. Jackson, G. J. Clowry, K. Vassilevski, A. OâNeill, and S. N. Baker, "The sinusoidal probe: a new approach to improve electrode longevity," *Frontiers in Neuroengineering*, Vol. 7, 2014.

61. Xie, C., J. Liu, T.-M. Fu, X. Dai, W. Zhou, and C. M. Lieber, "Three-dimensional macroporous nanoelectronic networks as minimally invasive brain probes," *Nature Materials*, Vol. 14, pp. 1286–1292, Dec. 2015.

62. Park, S., Y. Guo, X. Jia, H. K. Choe, B. Grena, J. Kang, J. Park, C. Lu, A. Canales, R. Chen, Y. S. Yim, G. B. Choi, Y. Fink, and P. Anikeeva, "One-step optogenetics with multifunctional flexible polymer fibers," *Nature Neuroscience*, Vol. 20, pp. 612–619, Apr. 2017.

63. Chung, T., J. Q. Wang, J. Wang, B. Cao, Y. Li, and S. W. Pang, "Electrode modifications to lower electrode impedance and improve neural signal recording sensitivity," *Journal of Neural Engineering*, Vol. 12, p. 056018, Sept. 2015.

64. Wang, Y., X. Yang, X. Zhang, Y. Wang, and W. Pei, "Implantable intracortical microelectrodes: reviewing the present with a focus on the future," *Microsystems & Nanoengineering*, Vol. 9, pp. 1–17, Jan. 2023.

65. Woo, H., S. Kim, H. Nam, W. Choi, K. Shin, K. Kim, S. Yoon, G. H. Kim, J. Kim, and G. Lim, "Au Hierarchical Nanostructure-Based Surface Modification of Microelectrodes for Improved Neural Signal Recording," *Analytical Chemistry*, Vol. 93, pp. 11765–11774, Aug. 2021.

66. Boehler, C., T. Stieglitz, and M. Asplund, "Nanostructured platinum grass enables superior impedance reduction for neural microelectrodes," *Biomaterials*, Vol. 67, pp. 346–353, Oct. 2015.

67. Bareket-Keren, L., and Y. Hanein, "Carbon nanotube-based multi electrode arrays for neuronal interfacing: progress and prospects," *Frontiers in neural circuits*, Vol. 6, p. 122, 2013.

68. Sim, S., H. Shin, K. Bae, H. Han, Y. Kang, J. Woo, Y. Cho, I.-J. Cho, and J. Kim, "Neural probe integrated with low-impedance electrodes implemented using vertically aligned carbon nanotubes for three-dimensional mapping of neural signals," *Sensors and Actuators B: Chemical*, Vol. 393, p. 134124, Oct. 2023.

69. Lu, Y., H. Lyu, A. G. Richardson, T. H. Lucas, and D. Kuzum, "Flexible Neural Electrode Array Based-on Porous Graphene for Cortical Microstimulation and Sensing," *Scientific Reports*, Vol. 6, p. 33526, Sept. 2016.

70. Desai, S. A., J. D. Rolston, L. Guo, and S. M. Potter, "Improving Impedance of Implantable Microwire Multi-Electrode Arrays by Ultrasonic Electroplating of Durable Platinum Black," *Frontiers in Neuroengineering*, Vol. 3, p. 5, May 2010.

71. Regehr, W., J. Pine, and D. Rutledge, "A long-term in vitro silicon-based microelectrode-neuron connection," *IEEE Transactions on Biomedical Engineering*, Vol. 35, pp. 1023–1032, Dec. 1988.

72. Zhang, C., J.-Q. Liu, H.-C. Tian, X.-Y. Kang, J.-C. Du, Y.-F. Rui, B. Yang, and C.-S. Yang, "Implantable electrode array with platinum black coating for brain stimulation in fish," *Microsystem Technologies*, Vol. 21, pp. 139–145, Jan. 2015.

73. Chen, C., S. Ruan, X. Bai, C. Lin, C. Xie, and I.-S. Lee, "Patterned iridium oxide film as neural electrode interface: Biocompatibility and improved neurite outgrowth with electrical stimulation," *Materials Science and Engineering: C*, Vol. 103, p. 109865, Oct. 2019.

74. Green, R., and M. R. Abidian, "Conducting Polymers for Neural Prosthetic and Neural Interface Applications," *Advanced materials (Deerfield Beach, Fla.)*, Vol. 27, pp. 7620–7637, Dec. 2015.

75. Balint, R., N. J. Cassidy, and S. H. Cartmell, "Conductive polymers: Towards a smart biomaterial for tissue engineering," *Acta Biomaterialia*, Vol. 10, pp. 2341–2353, June 2014.

76. Hassler, C., T. Boretius, and T. Stieglitz, "Polymers for neural implants," *Journal of Polymer Science Part B: Polymer Physics*, Vol. 49, no. 1, pp. 18–33, 2011.

77. Merrill, D. R., "Materials considerations of implantable neuroengineering devices for clinical use," *Current Opinion in Solid State and Materials Science*, Vol. 18, pp. 329–336, Dec. 2014.

78. Scholten, K., and E. Meng, "Materials for microfabricated implantable devices: a review," *Lab on a Chip*, Vol. 15, pp. 4256–4272, Oct. 2015.

79. Green, R. A., N. H. Lovell, and L. A. Poole-Warren, "Cell attachment functionality of bioactive conducting polymers for neural interfaces," *Biomaterials*, Vol. 30, pp. 3637–3644, Aug. 2009.

80. Cui, X., V. A. Lee, Y. Raphael, J. A. Wiler, J. F. Hetke, D. J. Anderson, and D. C. Martin, "Surface modification of neural recording electrodes with conducting polymer/biomolecule blends," *Journal of Biomedical Materials Research*, Vol. 56, pp. 261–272, Aug. 2001.

81. Thelin, J., H. Jörntell, E. Psouni, M. Garwicz, J. Schouenborg, N. Danielsen, and C. E. Linsmeier, "Implant Size and Fixation Mode Strongly Influence Tissue Reactions in the CNS," *PLOS ONE*, Vol. 6, no. 1, p. e16267, 2011.

82. Redolfi Riva, E., and S. Micera, "Progress and challenges of implantable neural interfaces based on nature-derived materials," *Bioelectronic Medicine*, Vol. 7, p. 6, Apr. 2021.

83. Shi, Y., R. Liu, L. He, H. Feng, Y. Li, and Z. Li, "Recent development of implantable and flexible nerve electrodes," *Smart Materials in Medicine*, Vol. 1, pp. 131–147, 2020.

84. Polikov, V. S., P. A. Tresco, and W. M. Reichert, "Response of brain tissue to chronically implanted neural electrodes," *Journal of Neuroscience Methods*, Vol. 148, no. 1, pp. 1–18, 2005.

85. Woeppel, K. M., X. S. Zheng, Z. M. Schulte, N. L. Rosi, and X. T. Cui, "Nanoparticle Doped PEDOT for Enhanced Electrode Coatings and Drug Delivery," *Advanced Healthcare Materials*, Vol. 8, no. 21, p. 1900622, 2019.

86. Antensteiner, M., M. Khorrami, F. Fallahianbijan, A. Borhan, and M. R. Abidian, "Conducting Polymer Microcups for Organic Bioelectronics and Drug Delivery Applications," *Advanced materials (Deerfield Beach, Fla.)*, Vol. 29, p. 10.1002/adma.201702576, Oct. 2017.

87. Moon, H. C., H. Choi, S. Kikionis, J. Seo, W. Youn, E. Ioannou, S. Y. Han, H. Cho, V. Roussis, and I. S. Choi, "Fabrication and Characterization of Neurocompatible Ulvan-Based Layer-by-Layer Films," *Langmuir*, Vol. 36, pp. 11610–11617, Oct. 2020.

88. Lee, J. Y., Z. Z. Khaing, J. J. Siegel, and C. E. Schmidt, "Surface modification of neural electrodes with a pyrrole-hyaluronic acid conjugate to attenuate reactive astrogliosis in vivo," *RSC Advances*, Vol. 5, pp. 39228–39231, Apr. 2015.

89. Ausilio, C., C. Lubrano, A. Mariano, and F. Santoro, "Negatively-charged supported lipid bilayers regulate neuronal adhesion and outgrowth," *RSC Advances*, Vol. 12, no. 47, pp. 30270–30277, 2023.

90. Huang, W.-C., H.-S. Chi, Y.-C. Lee, Y.-C. Lo, T.-C. Liu, M.-Y. Chiang, H.-Y. Chen, S.-J. Li, Y.-Y. Chen, and S.-Y. Chen, "Gene-Embedded Nanostructural BioticâAbiotic Optoelectrode Arrays Applied for Synchronous Brain Optogenetics and Neural Signal Recording," *ACS Applied Materials & Interfaces*, Vol. 11, pp. 11270–11282, Mar. 2019.

91. Kim, D.-H., J. Viventi, J. J. Amsden, J. Xiao, L. Vigeland, Y.-S. Kim, J. A. Blanco, B. Panilaitis, E. S. Frechette, D. Contreras, D. L. Kaplan, F. G. Omenetto, Y. Huang, K.-C. Hwang, M. R. Zakin, B. Litt, and J. A. Rogers, "Dissolvable Films of Silk Fibroin for Ultrathin, Conformal Bio-Integrated Electronics," *Nature materials*, Vol. 9, pp. 511–517, June 2010.

92. Patil, A. C., A. Bandla, Y.-H. Liu, B. Luo, and N. V. Thakor, "Nontransient silk sandwich for soft, conformal bionic links," *Materials Today*, Vol. 32, pp. 68–83, Jan. 2020.

93. Righi, M., G. L. Puleo, I. Tonazzini, G. Giudetti, M. Cecchini, and S. Micera, "Peptide-based coatings for flexible implantable neural interfaces," *Scientific Reports*, Vol. 8, p. 502, Jan. 2018.

94. Shen, W., S. Das, F. Vitale, A. Richardson, A. Ananthakrishnan, L. A. Struzyna, D. P. Brown, N. Song, M. Ramkumar, T. Lucas, D. K. Cullen, B. Litt, and M. G. Allen, "Microfabricated intracortical extracellular matrix-microelectrodes for improving neural interfaces," *Microsystems & Nanoengineering*, Vol. 4, pp. 1–15, Sept. 2018.

95. Togashi, H., T. Sakisaka, and Y. Takai, "Cell adhesion molecules in the central nervous system," *Cell Adhesion & Migration*, Vol. 3, no. 1, pp. 29–35, 2009.

96. Horstkorte, R., and B. Fuss, "Cell Adhesion Molecules," in *Basic Neurochemistry*, pp. 165–179, Elsevier, 2012.

97. Dalva, M. B., A. C. McClelland, and M. S. Kayser, "Cell adhesion molecules: signalling functions at the synapse," *Nature Reviews Neuroscience*, Vol. 8, pp. 206–220, Mar. 2007.

98. Harjunpää, H., M. Llort Asens, C. Guenther, and S. C. Fagerholm, "Cell Adhesion Molecules and Their Roles and Regulation in the Immune and Tumor Microenvironment," *Frontiers in Immunology*, Vol. 10, 2019.

99. Chooi, W. H., and S. Y. Chew, "Modulation of cell-cell interactions for neural tissue engineering: Potential therapeutic applications of cell adhesion molecules in nerve regeneration," *Biomaterials*, Vol. 197, pp. 327–344, Mar. 2019.

100. Gärtner, A., E. F. Fornasiero, S. Munck, K. Vennekens, E. Seuntjens, W. B. Huttner, F. Valtorta, and C. G. Dotti, "N-cadherin specifies first asymmetry in developing neurons: N-cadherin directs neuronal polarity," *The EMBO Journal*, Vol. 31, pp. 1893–1903, Apr. 2012.

101. Pielarski, K. N., B. van Stegen, A. Andreyeva, K. Nieweg, K. Jüngling, C. Redies, and K. Gottmann, "Asymmetric N-Cadherin Expression Results in Synapse Dysfunction, Synapse Elimination, and Axon Retraction in Cultured Mouse Neurons," *PLoS ONE*, Vol. 8, p. e54105, Jan. 2013.

102. Weledji, E. P., and J. C. Assob, "The ubiquitous neural cell adhesion molecule (N-CAM)," *Annals of Medicine and Surgery*, Vol. 3, pp. 77–81, Sept. 2014.

103. Cremer, H., G. Chazal, C. Goridis, and A. Represa, "NCAM Is Essential for Axonal Growth and Fasciculation in the Hippocampus," *Molecular and Cellular Neuroscience*, Vol. 8, no. 5, pp. 323–335, 1997.

104. Sridar, S., "Peptide modification of polyimide-insulated microwires: Towards improved biocompatibility through reduced glial scarring," *Acta Biomaterialia*, p. 13, 2017.

105. Krushel, L. A., O. Sporns, B. A. Cunningham, K. L. Crossin, and G. M. Edelman, "Neural cell adhesion molecule (N-CAM) inhibits astrocyte proliferation after injury to different regions of the adult rat brain.," *Proceedings of the National Academy of Sciences of the United States of America*, Vol. 92, pp. 4323–4327, May 1995.

106. Sporns, O., G. M. Edelman, and K. L. Crossin, "The neural cell adhesion molecule (N-CAM) inhibits proliferation in primary cultures of rat astrocytes.," *Proceedings of the National Academy of Sciences*, Vol. 92, pp. 542–546, Jan. 1995.

107. Haque, A., N. Adnan, A. Motazedian, F. Akter, S. Hossain, K. Kutsuzawa, K. Nag, E. Kobatake, and T. Akaike, "An Engineered N-Cadherin Substrate for Differentiation, Survival, and Selection of Pluripotent Stem Cell-Derived Neural Progenitors," *PLOS ONE*, Vol. 10, p. e0135170, Aug. 2015.

108. Lagenaur, C., and V. Lemmon, "An L1-like molecule, the 8D9 antigen, is a potent substrate for neurite extension.," *Proceedings of the National Academy of Sciences*, Vol. 84, pp. 7753–7757, Nov. 1987.

109. Walsh, F., K. Meiri, and P. Doherty, "Cell signalling and CAM-mediated neurite outgrowth.," *Society of General Physiologists series*, 1997.

110. Shin, M. H., E.-G. Lee, S.-H. Lee, Y. S. Lee, and H. Son, "Neural cell adhesion molecule (NCAM) promotes the differentiation of hippocampal precursor cells to a neuronal lineage, especially to a glutamatergic neural cell type," *Experimental & Molecular Medicine*, Vol. 34, pp. 401–410, Dec. 2002.

111. Neiiendam, J. L., L. B. KÃ¸hler, C. Christensen, S. Li, M. V. Pedersen, D. K. Ditlevsen, M. K. Kornum, V. V. Kiselyov, V. Berezin, and E. Bock, "An NCAM-derived FGF-receptor agonist, the FGL-peptide, induces neurite outgrowth and neuronal survival in primary rat neurons," *Journal of Neurochemistry*, Vol. 91, pp. 920–935, Nov. 2004.

112. Kohler, L. B., V. Soroka, I. Korshunova, V. Berezin, and E. Bock, "A peptide derived from a trans-homophilic binding site in neural cell adhesion molecule induces neurite outgrowth and neuronal survival," *Journal of Neuroscience Research*, Vol. 88, pp. 2165–2176, Aug. 2010.

113. Amoureux, M.-C., B. A. Cunningham, G. M. Edelman, and K. L. Crossin, "N-CAM Binding Inhibits the Proliferation of Hippocampal Progenitor Cells and Promotes Their Differentiation to a Neuronal Phenotype," *Journal of Neuroscience*, Vol. 20, pp. 3631–3640, May 2000.

114. Wiertz, R. W. F., E. Marani, and W. L. C. Rutten, "Neural cellâcell and cellâsubstrate adhesion through N-cadherin, N-CAM and L1," *Journal of Neural Engineering*, Vol. 8, p. 046004, Aug. 2011.

115. Arya, S. K., G. Chornokur, M. Venugopal, and S. Bhansali, "Dithiobis(succinimidyl propionate) modified gold microarray electrode based electrochemical immunosensor for ultrasensitive detection of cortisol," *Biosensors and Bioelectronics*, Vol. 25, pp. 2296–2301, June 2010.

116. Fairley, N., V. Fernandez, M. RichardâPlouet, C. Guillot-Deudon, J. Walton, E. Smith, D. Flahaut, M. Greiner, M. Biesinger, S. Tougaard, D. Morgan, and J. Baltrusaitis, "Systematic and collaborative approach to problem solving using X-ray photoelectron spectroscopy," *Applied Surface Science Advances*, Vol. 5, p. 100112, Sept. 2021.

117. Ouyang, Y., X. Cai, Q. Shi, L. Liu, D. Wan, S. Tan, and Y. Ouyang, "Poly-l-lysine-modified reduced graphene oxide stabilizes the copper nanoparticles with higher water-solubility and long-term additively antibacterial activity," *Colloids and Surfaces B: Biointerfaces*, Vol. 107, pp. 107–114, July 2013.

118. Riccardi, C. S., D. W. Hess, and B. Mizaikoff, "Surface-modified ZnSe waveguides for label-free infrared attenuated total reflection detection of DNA hybridization," *The Analyst*, Vol. 136, no. 23, p. 4906, 2011.

119. Ataman Sadik, D., H. Eksi-Kocak, G. Ertas, Ä. H. Boyaci, and M. Mutlu, "Mixed-monolayer of N-hydroxysuccinimide-terminated cross-linker and short alkanethiol to improve the efficiency of biomolecule binding for biosensing," *Surface and Interface Analysis*, Vol. 50, pp. 866–878, Sept. 2018.

120. Jiang, L., A. Glidle, A. Griffith, C. J. McNeil, and J. M. Cooper, "Characterising the formation of a bioelectrochemical interface at a self-assembled monolayer using X-ray photoelectron spectroscopy," *Bioelectrochemistry and Bioenergetics*, Vol. 42, pp. 15–23, Apr. 1997.

121. Ravi, S., S. Zhang, Y.-R. Lee, K.-K. Kang, J.-M. Kim, J.-W. Ahn, and W.-S. Ahn, "EDTA-functionalized KCC-1 and KIT-6 mesoporous silicas for Nd3+ ion recovery from aqueous solutions," *Journal of Industrial and Engineering Chemistry*, Vol. 67, pp. 210–218, Nov. 2018.

122. Varoni, E., E. Canciani, B. Palazzo, V. Varasano, P. Chevallier, L. Petrizzi, C. Dellavia, D. Mantovani, and L. Rimondini, "Effect of Poly-L-Lysine coating on titanium osseointegration: from characterization to in vivo studies," *Journal of Oral Implantology*, Vol. 41, pp. 626–631, Dec. 2015.

123. Noiset, O., Y.-J. Schneider, and J. Marchand-Brynaert, "Fibronectin adsorption or/and covalent grafting on chemically modified PEEK film surfaces," *Journal of Biomaterials Science, Polymer Edition*, Vol. 10, pp. 657–677, Jan. 1999.

124. Bilem, I., P. Chevallier, L. Plawinski, E. Sone, M. Durrieu, and G. Laroche, "RGD and BMP-2 mimetic peptide crosstalk enhances osteogenic commitment of human bone marrow stem cells," *Acta Biomaterialia*, Vol. 36, pp. 132–142, May 2016.

125. Liu, C., S. Z. Shen, and Z. Han, "Surface wettability and chemistry of ozone perfusion processed porous collagen scaffold," *Journal of Bionic Engineering*, Vol. 8, pp. 223–233, Sept. 2011.

126. Park, J. H., Z. Schwartz, R. Olivares-Navarrete, B. D. Boyan, and R. Tannenbaum, "Enhancement of Surface Wettability via the Modification of Microtextured Titanium Implant Surfaces with Polyelectrolytes," *Langmuir*, Vol. 27, pp. 5976–5985, May 2011.

127. Lim, C. Y., N. A. Owens, R. D. Wampler, Y. Ying, J. H. Granger, M. D. Porter, M. Takahashi, and K. Shimazu, "Succinimidyl Ester Surface Chemistry: Implications of the Competition between Aminolysis and Hydrolysis on Covalent Protein Immobilization," *Langmuir*, Vol. 30, pp. 12868–12878, Nov. 2014.

128. Guo, Y., F. Xia, L. Xu, J. Li, W. Yang, and L. Jiang, "Switchable Wettability on Cooperative Dual-Responsive Poly-l-lysine Surface," *Langmuir*, Vol. 26, pp. 1024–1028, Jan. 2010.

129. Vallèe, A., V. Humblot, C. MÃ©thivier, and C.-M. Pradier, "Glutathione adsorption from UHV to the liquid phase at various pH on gold and subsequent modification of protein interaction," *Surface and Interface Analysis*, Vol. 40, pp. 395–399, Mar. 2008.

130. Iucci, G., M. Dettin, C. Battocchio, R. Gambaretto, C. D. Bello, and G. Polzonetti, "Novel immobilizations of an adhesion peptide on the TiO2 surface: An XPS investigation," *Materials Science and Engineering: C*, Vol. 27, pp. 1201–1206, Sept. 2007.

131. Zhao, Q., Z. Yuan, Z. Duan, Y. Jiang, X. Li, Z. Li, and H. Tai, "An ingenious strategy for improving humidity sensing properties of multi-walled carbon nanotubes via poly-L-lysine modification," *Sensors and Actuators B: Chemical*, Vol. 289, pp. 182–185, June 2019.

132. Silva, W. M., H. Ribeiro, L. M. Seara, H. D. R. Calado, A. S. Ferlauto, R. M. Paniago, C. F. Leite, and G. G. Silva, "Surface properties of oxidized and aminated multi-walled carbon nanotubes," *Journal of the Brazilian Chemical Society*, Vol. 23, pp. 1078–1086, June 2012.

133. Rogers, S. L., P. C. Letourneau, S. L. Palm, J. McCarthy, and L. T. Furcht, "Neurite extension by peripheral and central nervous system neurons in response to substratum-bound fibronectin and laminin," *Developmental Biology*, Vol. 98, pp. 212–220, July 1983.

134. Clèment, J.-P., L. Al-Alwan, S. D. Glasgow, A. Stolow, Y. Ding, T. Quevedo Melo, A. Khayachi, Y. Liu, M. Hellmund, R. Haag, A. J. Milnerwood, P. Grütter, and T. E. Kennedy, "Dendritic Polyglycerol Amine: An Enhanced Substrate to Support Long-Term Neural Cell Culture," *ASN Neuro*, Vol. 14, p. 175909142110732, Jan. 2022.

135. Smith, T., "The hydrophilic nature of a clean gold surface," *Journal of Colloid and Interface Science*, Vol. 75, pp. 51–55, May 1980.

136. Enomoto, J., T. Kageyama, D. Myasnikova, K. Onishi, Y. Kobayashi, Y. Taruno, T. Kanai, and J. Fukuda, "Gold cleaning methods for preparation of cell culture surfaces for self-assembled monolayers of zwitterionic oligopeptides," *Journal of Bioscience and Bioengineering*, Vol. 125, pp. 606–612, May 2018.

137. Abeyratne-Perera, H. K., and P. L. Chandran, "Mannose Surfaces Exhibit Self-Latching, Water Structuring, and Resilience to Chaotropes: Implications for Pathogen Virulence," *Langmuir*, Vol. 33, pp. 9178–9189, Sept. 2017.

138. Ouerghi, O., M. F. Diouani, A. Belkacem, A. Elsanousi, and N. Jaffrezic-Renault, "Adjunction of Avidin to a Cysteamine Self-Assembled Monolayer for Impedimetric Immunosensor," *Journal of Biomaterials and Nanobiotechnology*, Vol. 07, no. 01, pp. 1–12, 2016.

139. Lin, D. W., C. J. Bettinger, J. P. Ferreira, C. L. Wang, and Z. Bao, "A Cell-Compatible Conductive Film from a Carbon Nanotube Network Adsorbed on Poly-L-Lysine," *ACS Nano*, Vol. 5, pp. 10026–10032, Dec. 2011.

140. Moron, C., A. Garcia, E. Tremps, and J. A. Somolinos, "Building Functional Surfaces for Biosensors Development," *Key Engineering Materials*, Vol. 543, pp. 204–207, Mar. 2013.

141. Arya, S. K., and P. Estrela, "Electrochemical immunosensor for tumor necrosis factor-alpha detection in undiluted serum," *Methods*, Vol. 116, pp. 125–131, Mar. 2017.

142. Buckley, C. D., G. E. Rainger, P. F. Bradfield, G. B. Nash, and D. L. Simmons, "Cell adhesion: More than just glue (Review)," *Molecular Membrane Biology*, Vol. 15, pp. 167–176, Jan. 1998.

143. Bremmer, F., S. Schallenberg, H. Jarry, S. Kuffer, S. Kaulfuss, P. Burfeind, A. Strauβ, P. Thelen, H. J. Radzun, P. Strobel, F. Honecker, and C. L. Behnes, "Role of N-cadherin in proliferation, migration, and invasion of germ cell tumours," *Oncotarget*, Vol. 6, pp. 33426–33437, Oct. 2015.

144. Edelman, G. M., and K. L. Crossin, "CELL ADHESION MOLECULES: Implications for a Molecular Histology," *Annual Review of Biochemistry*, Vol. 60, no. 1, pp. 155–190, 1991.

145. Sytnyk, V., I. Leshchynsâka, and M. Schachner, "Neural Cell Adhesion Molecules of the Immunoglobulin Superfamily Regulate Synapse Formation, Maintenance, and Function," *Trends in Neurosciences*, Vol. 40, pp. 295–308, May 2017.

146. Zamproni, L. N., M. T. V. V. Mundim, and M. A. Porcionatto, "Neurorepair and Regeneration of the Brain: A Decade of Bioscaffolds and Engineered Microtissue," *Frontiers in Cell and Developmental Biology*, Vol. 9, p. 649891, Apr. 2021.

147. Paradies, N. E., and G. B. Grunwald, "Purification and characterization of NCAD90, a Soluble endogenous form of N-cadherin, which is generated by proteolysis during retinal development and retains adhesive and neurite-promoting function," *Journal of Neuroscience Research*, Vol. 36, no. 1, pp. 33–45, 1993.

148. Haque, A., X.-S. Yue, A. Motazedian, Y.-i. Tagawa, and T. Akaike, "Characterization and neural differentiation of mouse embryonic and induced pluripotent stem cells on cadherin-based substrata," *Biomaterials*, Vol. 33, pp. 5094–5106, July 2012.

149. Shi, P., K. Shen, and L. C. Kam, "Local presentation of L1 and N-cadherin in multicomponent, microscale patterns differentially direct neuron function in vitro," *Developmental Neurobiology*, Vol. 67, no. 13, pp. 1765–1776, 2007.

150. Doherty, P., M. Fruns, P. Seaton, G. Dickson, C. H. Barton, T. A. Sears, and F. S. Walsh, "A threshold effect of the major isoforms of NCAM on neurite outgrowth," *Nature*, Vol. 343, pp. 464–466, Feb. 1990.

151. Meiri, K. F., J. L. Saffell, F. S. Walsh, and P. Doherty, "Neurite Outgrowth Stimulated by Neural Cell Adhesion Molecules Requires Growth-Associated Protein-43 (GAP-43) Function and Is Associated with GAP-43 Phosphorylation in Growth Cones," *Journal of Neuroscience*, Vol. 18, pp. 10429–10437, Dec. 1998.

152. Utton, M. A., B. Eickholt, F. V. Howell, J. Wallis, and P. Doherty, "Soluble N-cadherin stimulates fibroblast growth factor receptor dependent neurite outgrowth and N-cadherin and the fibroblast growth factor receptor co-cluster in cells," *Journal of Neurochemistry*, Vol. 76, no. 5, pp. 1421–1430, 2001.

153. Cherry, J. F., A. L. Carlson, F. L. Benarba, S. D. Sommerfeld, D. Verma, G. Loers, J. Kohn, M. Schachner, and P. V. Moghe, "Oriented, Multimeric Biointerfaces of the L1 Cell Adhesion Molecule: An Approach to Enhance Neuronal and Neural Stem Cell Functions on 2-D and 3-D Polymer Substrates," *Biointerphases*, Vol. 7, p. 22, Mar. 2012.

154. Roonprapunt, C., W. Huang, R. Grill, D. Friedlander, M. Grumet, S. Chen, M. Schachner, and W. Young, "Soluble Cell Adhesion Molecule L1-Fc Promotes Locomotor Recovery in Rats after Spinal Cord Injury," *Journal of Neurotrauma*, Vol. 20, pp. 871–882, Sept. 2003.

155. Esch, T., V. Lemmon, and G. Banker, "Differential effects of NgCAM and N-cadherin on the development of axons and dendrites by cultured hippocampal neurons," *Journal of Neurocytology*, Vol. 29, pp. 215–223, Mar. 2000.

156. Ditlevsen, D. K., G. K. Povlsen, V. Berezin, and E. Bock, "NCAM-induced intracellular signaling revisited," *Journal of Neuroscience Research*, Vol. 86, pp. 727–743, Mar. 2008.

157. Sponheim, C., V. Papadourakis, J. L. Collinger, J. Downey, J. Weiss, L. Pentousi, K. Elliott, and N. G. Hatsopoulos, "Longevity and reliability of chronic unit recordings using the Utah, intracortical multi-electrode arrays," *Journal of Neural Engineering*, Vol. 18, p. 066044, Dec. 2021.

158. Prasad, A., Q.-S. Xue, V. Sankar, T. Nishida, G. Shaw, W. J. Streit, and J. C. Sanchez, "Comprehensive characterization and failure modes of tungsten microwire arrays in chronic neural implants," *Journal of Neural Engineering*, Vol. 9, p. 056015, Oct. 2012.

159. Kolarcik, C. L., S. D. Luebben, S. A. Sapp, J. Hanner, N. Snyder, T. D. Y. Kozai, E. Chang, J. A. Nabity, S. T. Nabity, C. F. Lagenaur, and X. T. Cui, "Elastomeric and soft conducting microwires for implantable neural interfaces," *Soft Matter*, Vol. 11, no. 24, pp. 4847–4861, 2015.

160. Martins, J. P., P. Figueiredo, S. Wang, E. Espo, E. Celi, B. Martins, M. Kemell, K. Moslova, E. MÃ¤kilÃ¤, J. Salonen, M. A. Kostiainen, C. Celia, V. Cerullo, T. Viitala, B. Sarmento, J. Hirvonen, and H. A. Santos, "Neonatal Fc receptor-targeted lignin-encapsulated porous silicon nanoparticles for enhanced cellular interactions and insulin permeation across the intestinal epithelium," *Bioactive Materials*, Vol. 9, pp. 299–315, Mar. 2022.

161. Yang, K., J. Yang, W. Man, Z. Meng, C.-Y. Yang, Z. Cao, J. Liu, K. Kim, Y. Liu, S. Yang, Y. Guo, Z. He, C. Ma, G. Wang, and X. Wang, "N-Cadherin-Functionalized Nanofiber Hydrogel Facilitates Spinal Cord Injury Repair by Building a Favorable Niche for Neural Stem Cells," *Advanced Fiber Materials*, Mar. 2023.

162. Vega L., J. C. M., M. K. Lee, J. H. Jeong, C. E. Smith, K. Y. Lee, H. J. Chung, D. E. Leckband, and H. Kong, "Recapitulating CellâCell Adhesion Using N-Cadherin Biologically Tethered to Substrates," *Biomacromolecules*, Vol. 15, pp. 2172–2179, June.

163. Lemmon, V., S. M. Burden, H. R. Payne, G. J. Elmslie, and M. L. Hlavin, "Neurite growth on different substrates: permissive versus instructive influences and the role of adhesive strength," *Journal of Neuroscience*, Vol. 12, pp. 818–826, Mar. 1992.

164. Dihnè, M., C. Bernreuther, M. Sibbe, W. Paulus, and M. Schachner, "A New Role for the Cell Adhesion Molecule L1 in Neural Precursor Cell Proliferation, Differentiation, and Transmitter-Specific Subtype Generation," *Journal of Neuroscience*, Vol. 23, pp. 6638–6650, July 2003.

165. Lemmon, V., K. L. Farr, and C. Lagenaur, "L1-mediated axon outgrowth occurs via a homophilic binding mechanism," *Neuron*, Vol. 2, pp. 1597–1603, June 1989.

166. Kiryushko, D., V. Berezin, and E. Bock, "Regulators of Neurite Outgrowth: Role of Cell Adhesion Molecules," *Annals of the New York Academy of Sciences*, Vol. 1014, no. 1, pp. 140–154, 2004.

167. Williams, E. J., J. Furness, F. S. Walsh, and P. Doherty, "Activation of the FGF receptor underlies neurite outgrowth stimulated by L1, N-CAM, and N-cadherin," *Neuron*, Vol. 13, pp. 583–594, Sept. 1994.

168. Romano, N. H., C. M. Madl, and S. C. Heilshorn, "Matrix RGD ligand density and L1CAM-mediated Schwann cell interactions synergistically enhance neurite outgrowth," *Acta Biomaterialia*, Vol. 11, pp. 48–57, Jan. 2015.

169. Nielsen, J., K. Gotfryd, S. Li, N. Kulahin, V. Soroka, K. K. Rasmussen, E. Bock, and V. Berezin, "Role of Glial Cell Line-Derived Neurotrophic Factor (GDNF)âNeural Cell Adhesion Molecule (NCAM) Interactions in Induction of Neurite Outgrowth and Identification of a Binding Site for NCAM in the Heel Region of GDNF," *Journal of Neuroscience*, Vol. 29, pp. 11360–11376, Sept. 2009.

170. Lee, H. J., S. Bian, I. Jakovcevski, B. Wu, A. Irintchev, and M. Schachner, "Delayed Applications of L1 and Chondroitinase ABC Promote Recovery after Spinal Cord Injury," *Journal of Neurotrauma*, Vol. 29, pp. 1850–1863, July 2012.

171. Vara, H., and J. E. Collazos-Castro, "Biofunctionalized Conducting Polymer/Carbon Microfiber Electrodes for Ultrasensitive Neural Recordings," *ACS Applied Materials & Interfaces*, Vol. 7, pp. 27016–27026, Dec. 2015.

172. Xu, G., D. Y. Nie, W. Z. Wang, P. H. Zhang, J. Shen, B. T. Ang, G. H. Liu, X. G. Luo, N. L. Chen, and Z. C. Xiao, "Optic nerve regeneration in polyglycolic acidchitosan conduits coated with recombinant L1-Fc," *NeuroReport*, Vol. 15, p. 2167, Oct. 2004.

173. Wang, Y., S. Liu, H. Wang, Y. Zhao, and X.-D. Zhang, "Neuron devices: emerging prospects in neural interfaces and recognition," *Microsystems & Nanoengineering*, Vol. 8, pp. 1–13, Dec. 2022.

174. Doblado, L. R., C. Martìnez-Ramos, and M. M. Pradas, "Biomaterials for Neural Tissue Engineering," *Frontiers in Nanotechnology*, Vol. 3, 2021.

175. L, J. C. M. V., M. Kyung Lee, E. C. Qin, M. Rich, K. Young Lee, D. Hyun Kim, H. Jung Chung, D. E. Leckband, and H. Kong, "Three dimensional conjugation of recombinant N-cadherin to a hydrogel for in vitro anisotropic neural growth," *Journal of Materials Chemistry B*, Vol. 4, no. 42, pp. 6803–6811, 2016.

176. Rapeaux, A. B., and T. G. Constandinou, "Implantable brain machine interfaces: first-in-human studies, technology challenges and trends," *Current Opinion in Biotechnology*, Vol. 72, pp. 102–111, Dec. 2021.

177. Lee, S., A. J. Cortese, A. P. Gandhi, E. R. Agger, P. L. McEuen, and A. C. Molnar, "A 250 $\mu m \times 57 \mu m$ Microscale Opto-electronically Transduced Electrodes (MOTEs) for Neural Recording," *IEEE Transactions on Biomedical Circuits and Systems*, Vol. 12, pp. 1256–1266, Dec. 2018.

178. Seo, D., R. M. Neely, K. Shen, U. Singhal, E. Alon, J. M. Rabaey, J. M. Carmena, and M. M. Maharbiz, "Wireless Recording in the Peripheral Nervous System with Ultrasonic Neural Dust," *Neuron*, Vol. 91, pp. 529–539, Aug. 2016.

179. Maharbiz, M. M., R. Muller, E. Alon, J. M. Rabaey, and J. M. Carmena, "Reliable Next-Generation Cortical Interfaces for Chronic BrainâMachine Interfaces and Neuroscience," *Proceedings of the IEEE*, Vol. 105, pp. 73–82, Jan. 2017.

180. Sahel, J.-A., E. Boulanger-Scemama, C. Pagot, A. Arleo, F. Galluppi, J. N. Martel, S. D. Esposti, A. Delaux, J.-B. de Saint Aubert, C. de Montleau, E. Gutman, I. Audo, J. Duebel, S. Picaud, D. Dalkara, L. Blouin, M. Taiel, and B. Roska, "Partial recovery of visual function in a blind patient after optogenetic therapy," *Nature Medicine*, Vol. 27, pp. 1223–1229, July 2021.

181. Bertani, B., and N. Ruiz, "Function and biogenesis of lipopolysaccharides," *EcoSal Plus*, Vol. 8, no. 1, pp. 10–1128, 2018.

182. Kim, Y. H., N. S. Baek, Y. H. Han, M.-A. Chung, and S.-D. Jung, "Enhancement of neuronal cell adhesion by covalent binding of poly-d-lysine," *Journal of Neuroscience Methods*, Vol. 202, pp. 38–44, Oct. 2011.

183. Schildge, S., C. Bohrer, K. Beck, and C. Schachtrup, "Isolation and Culture of Mouse Cortical Astrocytes," *Journal of Visualized Experiments*, p. 50079, Jan. 2013.

184. Lu, Z., M. Piechowicz, and S. Qiu, "A Simplified Method for Ultra-Low Density, Long-Term Primary Hippocampal Neuron Culture," *Journal of Visualized Experiments*, p. 53797, Mar. 2016.

185. Ma, W., T. O'Shaughnessy, and E. Chang, "Cryopreservation of adherent neuronal networks," *Neuroscience Letters*, Vol. 403, pp. 84–89, July 2006.

186. Krasnow, S. M., J. G. Knoll, S. C. Verghese, P. R. Levasseur, and D. L. Marks, "Amplification and propagation of interleukin-1 βsignaling by murine brain endothelial and glial cells," *Journal of Neuroinflammation*, Vol. 14, p. 133, July 2017.

187. Hu, Y., G. Huang, J. Tian, J. Qiu, Y. Jia, D. Feng, Z. Wei, S. Li, and F. Xu, "Matrix stiffness changes affect astrocyte phenotype in an in vitro injury model," *NPG Asia Materials*, Vol. 13, p. 35, Dec. 2021.

188. Moeendarbary, E., I. P. Weber, G. K. Sheridan, D. E. Koser, S. Soleman, B. Haenzi, E. J. Bradbury, J. Fawcett, K. Franze, I. P. Weber, G. K. Sheridan, D. E. Koser, S. Soleman, B. Haenzi, E. J. Bradbury, J. Fawcett, and K. Franze, "The soft mechanical signature of glial scars in the central nervous system," *Nature Communications*, Vol. 8, p. 14787, Mar. 2017.

189. Jha, M. K., J.-H. Kim, G. J. Song, W.-H. Lee, I.-K. Lee, H.-W. Lee, S. S. A. An, S. Kim, and K. Suk, "Functional dissection of astrocyte-secreted proteins: Implications in brain health and diseases," *Progress in Neurobiology*, Vol. 162, pp. 37–69, Mar. 2018.

190. Chen, Q., Z. Liang, Q. Yue, X. Wang, S. W. I. Siu, M. Pui-Man Hoi, and S. M.-Y. Lee, "A Neuropeptide Y/F-like Polypeptide Derived from the Transcriptome of Turbinaria peltata Suppresses LPS-Induced Astrocytic Inflammation," *Journal of Natural Products*, Vol. 85, pp. 1569–1580, June 2022.

191. ELBini, I., and N.-e. Neili, "Potassium channels at the crossroads of neuroinflammation and myelination in experimental models of multiple sclerosis," *Biochemical and Biophysical Research Communications*, Vol. 653, pp. 140–146, Apr. 2023.

192. Singh, D., A. Agrawal, C. M. S. Singal, H. S. Pandey, P. Seth, and S. K. Sharma, "Sinomenine inhibits amyloid beta-induced astrocyte activation and protects neurons against indirect toxicity," *Molecular Brain*, Vol. 13, p. 30, Mar. 2020.

193. Hawkins, B. T., S. Grego, and K. L. Sellgren, "Three-dimensional culture conditions differentially affect astrocyte modulation of brain endothelial barrier function in response to transforming growth factor β1," *Brain Research*, Vol. 1608, pp. 167–176, May 2015.

194. Freeman, R., M. Han, Z. Álvarez, J. A. Lewis, J. R. Wester, N. Stephanopoulos, M. T. McClendon, C. Lynsky, J. M. Godbe, H. Sangji, *et al.*, "Reversible self-assembly of superstructured networks," *Science*, Vol. 362, no. 6416, pp. 808–813, 2018.

195. Pogoda, K., and P. A. Janmey, "Glial tissue mechanics and mechanosensing by glial cells," *Frontiers in cellular neuroscience*, Vol. 12, p. 25, 2018.

196. East, E., N. Johns, M. Georgiou, J. P. Golding, A. J. Loughlin, P. J. Kingham, and J. B. Phillips, "A 3D in vitro model reveals differences in the astrocyte response elicited by potential stem cell therapies for CNS injury," *Regenerative Medicine*, Vol. 8, pp. 739–746, Nov. 2013.

197. East, E., J. P. Golding, and J. B. Phillips, "A versatile 3D culture model facilitates monitoring of astrocytes undergoing reactive gliosis," *Journal of Tissue Engineering and Regenerative Medicine*, Vol. 3, pp. 634–646, Dec. 2009.